

Contract No:

This document was prepared in conjunction with work accomplished under Contract No. DE-AC09-08SR22470 with the U.S. Department of Energy (DOE) Office of Environmental Management (EM).

Disclaimer:

This work was prepared under an agreement with and funded by the U.S. Government. Neither the U. S. Government or its employees, nor any of its contractors, subcontractors or their employees, makes any express or implied:

- 1) warranty or assumes any legal liability for the accuracy, completeness, or for the use or results of such use of any information, product, or process disclosed; or
- 2) representation that such use or results of such use would not infringe privately owned rights; or
- 3) endorsement or recommendation of any specifically identified commercial product, process, or service.

Any views and opinions of authors expressed in this work do not necessarily state or reflect those of the United States Government, or its contractors, or subcontractors.

Contract No:

This document was prepared in conjunction with work accomplished under Contract No. DE-AC09-08SR22470 with the U.S. Department of Energy (DOE) Office of Environmental Management (EM).

Disclaimer:

This work was prepared under an agreement with and funded by the U.S. Government. Neither the U. S. Government or its employees, nor any of its contractors, subcontractors or their employees, makes any express or implied:

- 1) warranty or assumes any legal liability for the accuracy, completeness, or for the use or results of such use of any information, product, or process disclosed; or
- 2) representation that such use or results of such use would not infringe privately owned rights; or
- 3) endorsement or recommendation of any specifically identified commercial product, process, or service.

Any views and opinions of authors expressed in this work do not necessarily state or reflect those of the United States Government, or its contractors, or subcontractors.



Savannah River
National Laboratory®

A U.S. DEPARTMENT OF ENERGY NATIONAL LABORATORY • SAVANNAH RIVER SITE • AIKEN, SC

Hydraulic Testing of the Lost Lake Aquifer Near Recovery Well RWM019

K. L. Dixon

March 2021

SRNL-STI-2021-00026, Revision 0

SRNL.DOE.GOV

DISCLAIMER

This work was prepared under an agreement with and funded by the U.S. Government. Neither the U.S. Government or its employees, nor any of its contractors, subcontractors or their employees, makes any express or implied:

1. warranty or assumes any legal liability for the accuracy, completeness, or for the use or results of such use of any information, product, or process disclosed; or
2. representation that such use or results of such use would not infringe privately owned rights; or
3. endorsement or recommendation of any specifically identified commercial product, process, or service.

Any views and opinions of authors expressed in this work do not necessarily state or reflect those of the United States Government, or its contractors, or subcontractors.

Printed in the United States of America

**Prepared for
U.S. Department of Energy**

Keywords: *Environmental
Hydraulic Conductivity*

Retention: *Permanent*

Hydraulic Testing of the Lost Lake Aquifer Near Recovery Well RWM019

K. L. Dixon

March 2021



Prepared for the U.S. Department of Energy under
contract number DE-AC09-08SR22470.

OPERATED BY SAVANNAH RIVER NUCLEAR SOLUTIONS

REVIEWS AND APPROVALS

AUTHORS:

K. L. Dixon, SRNL Environmental Sciences and Dosimetry Date

TECHNICAL REVIEW:

S. A. Goodlove, SRNL Environmental Sciences and Dosimetry Date

APPROVAL:

D. G. Jackson, Manager
SRNL Environmental Sciences and Dosimetry Date

B. J. Kramer, EC&ACP Engineering Date

J. E. Cardoso-Neto, EC&ACP Project Management Date

EXECUTIVE SUMMARY

An aquifer pumping test was conducted on the Lost Lake Aquifer Zone (LLAZ) at the recently installed recovery well RWM019 in accordance with the approved test plan (Dixon, 2020). The objective of the testing was to determine baseline well performance parameters and aquifer hydraulic conductivity. This testing consisted of a step-drawdown test to determine well performance properties, a constant pumping rate aquifer test to determine aquifer hydraulic properties, and a post-test aquifer recovery monitoring period also used to estimate aquifer hydraulic properties. Well performance parameters determined included specific capacity, well efficiency, and head loss coefficients. The specific capacity of RWM019 was determined to be approximately 2.6 gpm/ft of drawdown based on the final step of the step-drawdown test. Well efficiency was inversely related to pumping rate and decreased from 87% to 81% over a pumping range of approximately 49 to 79 gpm. The aquifer head loss coefficient was determined to be 2.3 ft/ft³/min and the well loss coefficient was determined to be 0.05 min²/ft⁵.

Aquifer response to pumping at RWM019 was measured in several nearby observation wells screened within the LLAZ. Drawdown data were collected during the step-drawdown test and during the constant rate pumping test. Recovery data were also collected following shutdown of RWM019. These data were used to evaluate aquifer hydraulic properties using the Hantush-Jacob (1955, 1961a, and b) leaky aquifer model as implemented in the computer code AQTESOLV (Table ES1). The average transmissivity (T) of the aquifer based on all testing was determined to be 1.87 ft²/min with a standard deviation of 0.74 ft²/min. The average storativity of the aquifer was determined to be 0.001 with a standard deviation of 0.0012. The average hydraulic conductivity of the LLAZ near RWM019 was determined to be 43.9 ft/day with a standard deviation of 16.8 ft/day. The average hydraulic conductivity of the overlying confining layer, the green clay confining unit (GCCZ) was determined to be 0.002 ft/day with a standard deviation of 0.0024 ft/ day.

At the time the original recovery well network was installed, extensive hydraulic testing was conducted to determine aquifer hydraulic properties. Of the recovery wells in the original network, RWM 7 and RWM 10 are the closest to RWM019. The transmissivity of the aquifer at RWM 7

and RWM 10 was reported as 1.95 and 2.32 ft²/min, respectively (Geraghty and Miller, 1987). The results from the testing of RWM019 are comparable to the previous testing and suggest the aquifer is more transmissive in this area than near RWM018 where a transmissivity of 0.816 ft²/min was measured (Dixon, 2018).

Table ES1. Average Hydraulic Properties of the Lost Lake Aquifer near RWM019^a

	Transmissivity (ft ² /min)	Hydraulic Conductivity (ft/day)	Storativity	r/B	Green Clay Hydraulic Conductivity (ft/day)
Average	1.8656	43.9	0.0010	0.2146	1.7E-03
Median	1.7780	42.7	0.0007	0.1018	3.1E-04
Standard Deviation	0.7439	16.8	0.0012	0.2534	2.4E-03

^aBased on data from step-drawdown testing and constant rate aquifer testing.

TABLE OF CONTENTS

LIST OF TABLES	viii
LIST OF FIGURES.....	viii
LIST OF ABBREVIATIONS.....	xi
1.0 Introduction.....	1
2.0 Hydrologic Test Methods and Objectives.....	2
2.1 Review of Previous Aquifer Testing Near RWM019	2
2.2 Hydrogeologic Conceptual Model	3
2.3 Step Drawdown Pumping Tests.....	3
2.4 Aquifer Pumping Test	4
2.5 Analysis of Pumping Test Data	5
2.6 Barometric Effects	8
3.0 Results.....	9
3.1 Barometric Efficiency	9
3.2 Step Drawdown Testing	10
3.3 RWM019 Aquifer Test.....	11
3.4 Analysis of LLAZ Hydraulic Properties	13
3.4.1 Analysis of Step-Drawdown Test Data.....	13
3.4.2 Analysis of Constant Rate Aquifer Test Data	14
3.4.3 Analysis of Aquifer Response to RWM 1.....	15
3.4.4 Summary of Hydraulic Properties	16
3.5 Verification Calculations.....	16
4.0 Conclusions.....	17
5.0 References.....	19

LIST OF TABLES

Table 1. Previously Reported Hydraulic Properties of the Lost Lake Aquifer Zone	52
Table 2 Construction Details for Wells Used in Aquifer Test at RWM019	53
Table 3. Calculated Barometric Efficiencies for RWM019 and Nearby Observation Wells.....	54
Table 4. Specific Capacity and Efficiencies Calculated for RWM019.....	54
Table 5. Well Loss Parameters Calculated for RWM019.....	55
Table 6 Aquifer Response to Step-Drawdown Test at RWM019	55
Table 7. Maximum Drawdown as a Function of Days Since Start of Pumping for RWM019 Constant Rate Aquifer Test.....	56
Table 8 Flow Data from Recovery Well Network During Constant Rate Aquifer Test (as determined from ACP round sheets).....	56
Table 9 RWM 1 Shutdown History.....	57
Table 10: Relative Well Dimensions Used in AQTESOLV Analysis of RWM019 Pumping Test Data...	57
Table 11 Hydraulic Properties of the Lost Lake Aquifer Based on Step-Drawdown Test at RWM019 ..	58
Table 12 Hydraulic Properties of the Lost Lake Aquifer Based on Constant Rate Pumping Test at RWM019.....	59
Table 13. Average Hydraulic Properties of the Lost Lake Aquifer Near RWM019.....	60

LIST OF FIGURES

Figure 1. Location of Recovery Wells.....	21
Figure 2. Location of Recovery Well RWM019 and Nearby Monitoring Wells.....	22
Figure 3: Generalized Lithologic Cross Section Near RWM019.....	23
Figure 4. Screen Elevations for RWM019 Aquifer Test Wells.....	24
Figure 5: Plot for Calculating Formation Loss Coefficient B and Well Lose Coefficient C from Step Drawdown Tests (adapted from Spane and Newcomer, 2007).....	25
Figure 6: Effect of Barometric Efficiency Corrections to Water Level Data from MSB 14A.....	25
Figure 7: Effect of Barometric Efficiency Corrections to Water Level Data from MSB 14B.....	26
Figure 8. Drawdown as a Function of Time for RWM019 Step Test.....	26
Figure 9. Specific Discharge as a Function of Pumping Rate for RWM019.	27
Figure 10. Well Efficiency as a Function of Pumping Rate for RWM019.....	27

Figure 11. Head Loss Plot for Step-Drawdown Test at RWM019.....	28
Figure 12. Head Loss Plot for RWM019.....	28
Figure 13. Step Test Drawdown Data and Hantush-Jacob Leaky Aquifer Type Curve for MSB 14A....	29
Figure 14. Step Test Drawdown Data and Hantush-Jacob Leaky Aquifer Type Curve for MSB 14B....	29
Figure 15. Step Test Drawdown Data and Hantush-Jacob Leaky Aquifer Type Curve for MSB 1C.....	30
Figure 16. Step Test Drawdown Data and Hantush-Jacob Leaky Aquifer Type Curve for MSB002BR..	30
Figure 17. Step Test Drawdown Data and Hantush-Jacob Leaky Aquifer Type Curve for MSB002CR..	31
Figure 18. Step Test Drawdown Data and Hantush-Jacob Leaky Aquifer Type Curve for MSB003CR..	31
Figure 19. Step Test Drawdown Data and Hantush-Jacob Leaky Aquifer Type Curve for MSB004BR..	32
Figure 20. Step Test Drawdown Data and Hantush-Jacob Leaky Aquifer Type Curve for MSB004CR..	32
Figure 21. Step Test Drawdown Data and Hantush-Jacob Leaky Aquifer Type Curve for MSB39B....	33
Figure 22. Step Test Drawdown Data and Hantush-Jacob Leaky Aquifer Type Curve for MSB63B....	33
Figure 23. RWM019 Flow Rate During Constant Pumping Rate Aquifer Test.....	34
Figure 24. Drawdown as a Function of Elapsed Time for MSB 14A.....	35
Figure 25. Drawdown as a Function of Elapsed Time for MSB 14B.....	35
Figure 26. Drawdown as a Function of Elapsed Time for MSB 1C.....	36
Figure 27. Drawdown as a Function of Elapsed Time for MSB002BR.....	36
Figure 28. Drawdown as a Function of Elapsed Time for MSB002CR ..	37
Figure 29. Drawdown as a Function of Elapsed Time for MSB003BR ..	37
Figure 30. Drawdown as a Function of Elapsed Time for MSB003CR ..	38
Figure 31. Effect of RWM 1 Shutdown/Restart on MSB003CR ..	38
Figure 32. Drawdown as a Function of Elapsed Time for MSB004BR ..	39
Figure 33. Drawdown as a Function of Elapsed Time for MSB004CR ..	39
Figure 34. Effect of RWM 1 Shutdown/Restart on MSB004CR ..	40
Figure 35. Drawdown as a Function of Elapsed Time for MSB 39B ..	40
Figure 36. Drawdown as a Function of Elapsed Time for MSB 63B ..	41
Figure 37. Influence of Unidentified Well on Drawdown at MSB 63B ..	41
Figure 38. Drawdown as a Function of Elapsed Time for SSM029B ..	42
Figure 39. Influence of Unidentified Well on Drawdown at SSM029B ..	42

Figure 40. Drawdown Data and Hantush-Jacob Leaky Aquifer Type Curve for MSB14A	43
Figure 41. Drawdown Data and Hantush-Jacob Leaky Aquifer Type Curve for MSB14B.....	43
Figure 42. Drawdown Data and Hantush-Jacob Leaky Aquifer Type Curve for MSB1C.....	44
Figure 43. Drawdown Data and Hantush-Jacob Leaky Aquifer Type Curve for MSB002BR.....	44
Figure 44. Drawdown Data and Hantush-Jacob Leaky Aquifer Type Curve for MSB002CR.....	45
Figure 45. Drawdown Data and Hantush-Jacob Leaky Aquifer Type Curve for MSB003BR.....	45
Figure 46. Drawdown Data and Hantush-Jacob Leaky Aquifer Type Curve for MSB003CR.....	46
Figure 47. Drawdown Data and Hantush-Jacob Leaky Aquifer Type Curve for MSB004BR.....	46
Figure 48. Drawdown Data and Hantush-Jacob Leaky Aquifer Type Curve for MSB004CR.....	47
Figure 49. Drawdown Data and Hantush-Jacob Leaky Aquifer Type Curve for MSB 39B.....	47
Figure 50. Drawdown Data and Hantush-Jacob Leaky Aquifer Type Curve for MSB 63B.....	48
Figure 51. Drawdown Data and Hantush-Jacob Leaky Aquifer Type Curve for SSM029B	48
Figure 52. Drawdown Data and Hantush-Jacob Leaky Aquifer Type Curve for MSB003CR with RWM 1 as Pumping Well.....	49
Figure 53. Drawdown Data and Hantush-Jacob Leaky Aquifer Type Curve for MSB004CR with RWM 1 as Pumping Well.....	49
Figure 54. Cumulative Probability Plot of Transmissivity for the Lost Lake Aquifer Near RWM019....	50
Figure 55. Probability Density Function for Transmissivity of the Lost Lake Aquifer Near RWM019....	50
Figure 56. Drawdown as a Function of Time for MSB 14A Using Theis Solution (spreadsheet calculation for verification).	51
Figure 57. Comparison of Measured and Predicted Drawdown.	51

LIST OF ABBREVIATIONS

~	approximate, approximately
B	Linear head loss coefficient
C	Non-linear (turbulent) well loss coefficient
EC&ACP	Environmental Compliance and Area Completion Projects
CBCU	Crouch Branch Confining Unit
GCCZ	Green Clay Confining Unit
gpm	gallons per minute
HWMF	Hazardous Waste Management Facility
LLAZ	Lost Lake Aquifer Zone
P	Order of non-linear well loss
PCE	Perchloroethylene
PVC	Polyvinyl Chloride
Q	Pumping rate
S	Storativity
SCDHEC	South Carolina Department of Health and Environmental Control
SRNL	Savannah River National Laboratory
SRS	Savannah River Site
Sw	Wellbore skin factor
T	Transmissivity
TCE	Trichloroethylene
UIC	Underground Injection Control Permit
VOC	Volatile Organic Compound

1.0 Introduction

Groundwater beneath the M-Area Hazardous Waste Management Facility (HWMF) is contaminated with volatile organic compounds (VOC) including trichloroethylene (TCE) and tetrachloroethylene (PCE). SRS operates a network of recovery wells designed to hydraulically contain and capture the high concentration VOC plume in the LLAZ (Figure 1). The recovery wells are connected to the M-1 Air Stripper and the system is permitted by the South Carolina Department of Environmental Control (SCDHEC) to operate at a total flow of 610 gpm. RWM019 was installed to target the higher concentration area of dissolved VOC plume that is outside of the zone of capture of the M-1 Air Stripper recovery wells.

Although modified over time, the original recovery well network was installed in the 1980s. Extensive aquifer testing was conducted using the original well network and estimates of specific capacity, well efficiency, transmissivity, and storage coefficient were made for the LLAZ (Geraghty and Miller, 1987). Results from previous testing are summarized in Table 1. Transmissivities for the LLAZ ranged from 0.344 to 9.28 ft²/min (using constant rate drawdown tests). More recently, aquifer testing was conducted at RWM018, RWM 3, RWM 5, and RWM 8. For the LLAZ near RWM018, transmissivity ranged from 0.660 to 1.086 ft²/min with an average of 0.816 ft²/min (Dixon, 2018). Near RWM 3 and RWM 5, LLAZ transmissivity was estimated be 0.992 ft²/min. For the LLAZ near RWM 8, transmissivity ranged from 0.715 to 1.167 ft²/min with an average of 0.946 ft²/min (Dixon, 2019). Of the recovery wells in the original network, RWM 7 and RWM 10 are the closest to RWM019. The transmissivity of the aquifer at RWM 7 and RWM 10 was reported as 1.95 and 2.32 ft²/min, respectively (Geraghty and Miller. 1987).

Installation of RWM019 provided an opportunity to obtain current hydrologic property information about the LLAZ in the vicinity of the recovery well. As a result, tests were designed to determine specific well performance parameters for RWM019 (e.g., specific capacity, well efficiency, and head loss coefficients) and to determine aquifer hydraulic properties (e.g., transmissivity and storativity). Hydrologic tests included step-drawdown testing of RWM019 and a longer duration constant rate pumping test where water levels were monitored in several nearby monitoring wells.

This report discusses the hydrologic tests conducted following the installation of RWM019. The information provided in this report may serve as input to subsequent updates to the groundwater flow and contaminant transport model for A/M Area.

2.0 Hydrologic Test Methods and Objectives

The objectives of this testing were to determine the specific capacity, efficiency, and pumping capacity of RWM019 and to estimate aquifer hydraulic properties including transmissivity and storativity. These objectives were met by conducting a step-drawdown test and a constant rate aquifer pumping test. Testing at RWM019 was conducted with the other wells in the recovery network operating at near steady-state conditions. This was done so that any observed aquifer response could be attributed to testing at RWM019. The following sections describe the test methods used to meet the project objectives.

2.1 Review of Previous Aquifer Testing Near RWM019

At the time of installation (circa 1984) of the recovery well network, several step-drawdown and aquifer pumping tests were conducted in order to estimate the performance properties of the recovery wells and the hydraulic properties of the LLAZ. The results of this work are presented by Geraghty and Miller (1987) and are summarized in Table 1. The closest recovery wells to RWM019 are RWM 7 and RWM 10. RWM 7 is located 717 ft to the east of RWM019 whereas RWM 10 is located 654 ft northwest of RWM019 (Figure 1). A transmissivity of $1.95 \text{ ft}^2/\text{min}$ ($K = 46.8 \text{ ft/day}$, $b = 60 \text{ ft}$) and storativity of 0.0006 was reported for RWM 7. A transmissivity of $2.32 \text{ ft}^2/\text{min}$ ($K = 55.7 \text{ ft/day}$, $b = 60 \text{ ft}$) and storativity of 0.0009 was reported for RWM 10.

In 2018, aquifer testing was conducted at RWM018 (Dixon, 2018). Transmissivity near RWM018 was estimated to be $0.816 \text{ ft}^2/\text{min}$ and storativity was estimated to be 0.00047. From the results of the RWM018 testing, specific capacity of RWM018 was estimated to be 3.2 gpm/ft with an estimated maximum pumping rate between 85 and 100 gpm (Dixon, 2018). Aquifer testing was also conducted near RWM 3 and RWM 5 (Dixon, 2018). Transmissivity was estimated to be $0.992 \text{ ft}^2/\text{min}$ and storativity was estimated to be 0.001. Further away at RWM 16, Hiergessell (1992) conducted testing of the LLAZ and found the transmissivity to range from 0.782 to $0.899 \text{ ft}^2/\text{min}$ and storativity to range from 0.0005 to 0.0007.

2.2 Hydrogeologic Conceptual Model

The location of RWM019 and nearby monitoring wells is shown in Figure 2 and a generalized north-south geologic cross-section is given in Figure 3. A detailed description of the hydrostratigraphic setting in A/M area is provided by (Aadland and Bledsoe, 1990) and details pertinent to this test are summarized here. The generalized hydrostratigraphy pertinent to the study area consists of: 1) the M-Area aquifer zone (MAAZ), 2) the GCCZ, 3) the LLAZ, and 4) the upper clay of the Crouch Branch Confining Unit (UC_CBCU).

The MAAZ is the water table aquifer and it overlies the GCCZ. The GCCZ ranges in thickness from about 4 to 12 ft across the RWM019 study area, with a thickness of 4 ft at RWM019. The GCCZ serves as the leaky confining layer in the subsequent analysis of RWM019 pumping test data. The LLAZ ranges in thickness from about 45 to 70 ft across the study area with a thickness of 54 ft at RWM019. The LLAZ is bounded on the bottom by the UC_CBCU.

2.3 Step Drawdown Pumping Tests

Step-drawdown tests are conducted to assess well performance and to identify the optimum pumping rate for a recovery well. A step-drawdown test is conducted as a series of short duration, constant-rate pumping tests consisting of a minimum of three steps that are of approximate equal duration (Kruseman and Ritter, 1994). This approach was used for a step-drawdown test conducted at RWM019. The test was conducted at flow rates of about 49, 64, and 79 gpm. Due to an obstruction in RWM019 (~140 feet below ground surface (ft bgs)), it was not possible to insert a pressure transducer to monitor the response to the step-test. Therefore, water levels in RWM019 were manually recorded during the test using a water level tape. Flow rates were also manually recorded. Each individual pumping period lasted for approximately 120 minutes. Following the completion of the final step, pumping was terminated. Recovery of the pumping well was monitored, and these data were included in the analysis.

The specific capacity of a pumping well is defined as discharge per unit drawdown (Q/s) as measured in the pumping well (Kruseman and Ritter, 1994). It provides an indicator of initial well performance and is useful in quantifying subsequent declines in performance over time that may arise as pumping progresses. The specific capacity of RWM019 was assessed by plotting drawdown as a function of discharge for each pumping interval.

Head loss coefficients for RWM019 were determined by comparing discharge, Q , to the ratio of drawdown and pumping rate (s/Q). The ratio s/Q is defined as specific discharge. Jacob (1946) defined the relationship between well loss and drawdown as follows:

$$s_t = BQ + CQ^2 \quad (2-1)$$

where s_t is the total drawdown, BQ is the laminar aquifer head loss, and CQ^2 is the turbulent well head loss. A plot of specific discharge as a function of pumping rate provides the coefficients B and C (Figure 5).

Well efficiency is the ratio of the theoretical drawdown (without well losses) expected in a pumping well and the observed drawdown in the well. Efficiency is calculated directly using this ratio if estimates of transmissivity and storativity are available. Efficiency may also be calculated from Equation 2-1 as follows:

$$E = \frac{BQ}{BQ + CQ^2} * 100 \quad (2-2)$$

This is simply the aquifer head loss divided by the total head loss in the well. Simplifying Equation 2-2 gives:

$$E = \frac{100}{1 + \frac{CQ}{B}} \quad (2-3)$$

where B is the aquifer head loss coefficient and C is the well loss coefficient.

2.4 Aquifer Pumping Test

Following the step-drawdown test, a constant rate aquifer pumping test was conducted at RWM019. Water was pumped from RWM019 at a relatively constant flow rate of about 79 gpm for the duration of the test activities. During the pumping test at RWM019, the system configuration (recovery wells in use and pumping rates) was maintained as close to constant as possible so that the measured aquifer response could be attributed to RWM019.

An extensive monitoring well network exists near RWM019 and several of those wells are screened in the LLAZ. A subset of these wells were used to monitor aquifer response due to pumping at RWM019 (Figure 2 and Table 2). Figure 4 shows a plot of screen intervals for RWM019 compared to the monitoring wells chosen for this test.

For both the step-drawdown and aquifer pumping tests, vented, data logging pressure transducers were used to monitor aquifer response. Pressure transducers are submerged below the water column in the well and record the pressure due to the weight of the water column above the transducer. Changes in water level result in a change in pressure sensed by the transducer. The pressure measured by the transducer was recorded in feet of water above the sensor. These data were converted to elevation using the initial water level in the well (manually recorded using an electric water level tape) and the reference elevation for the top of casing. Barometric pressure was monitored continuously near RWM019 (In-Situ, Inc., Barotroll).

RWM019 is equipped with a direct reading flow meter and pressure gauge. In addition to the LCD display, the flow meter outputs a signal for logging pumping rate. For the aquifer pumping test, the pumping rate of RWM019 was recorded using a data logger (Onset Inc., HOBO U12-008).

2.5 Analysis of Pumping Test Data

The LLAZ is considered a leaky confined aquifer being bounded by the GCCZ at the top and UC_CBCU on the bottom. The GCCZ in M-Area has been described as discontinuous (Marine and Bledsoe, 1984) and identified as a leaky confining layer (Dixon, 2018; Dixon, 2019; Hiergesell, 1992). Therefore, the method chosen for analyzing the bulk of data from the aquifer pumping tests considers leakage from an overlying confining layer. Initial estimates of aquifer properties were made using the Theis solution for confined aquifers (Theis, 1935).

The Theis equation is given as:

$$s = \frac{Q}{4\pi T} \int_u^{\infty} \frac{e^{-y}}{y} dy \quad (2-4)$$

where s is drawdown in the aquifer, Q is the pumping rate (Fetter, 1994). The parameter u is given as:

$$u = \frac{r^2 S}{4 T t} \quad (2-5)$$

where r is the radial distance from the pumping well, S is the storativity of the aquifer, T is the transmissivity of the aquifer, and t is the time since pumping started.

Equation 2-4 is typically abbreviated as:

$$s = \frac{Q}{4\pi T} W(u) \quad (2-6)$$

where $W(u)$ is referred to as the Theis well function (Chow, 1964).

The Theis well function $W(u)$ is given as:

$$W(u) = -0.5772 - \ln(u) + u - \frac{u^2}{2 * 2!} + \frac{u^3}{3 * 3!} - \frac{u^4}{4 * 4!} + \dots \quad (2-7)$$

Assumptions associated with the Theis method include:

- The aquifer has infinite areal extent
- aquifer is homogeneous and of uniform thickness
- the pumping well is fully or partially penetrating
- flow to the pumping well is horizontal when the pumping well is fully penetrating

- aquifer is nonleaky confined
- flow is unsteady
- water is released instantaneously from storage with decline of hydraulic head
- diameter of a pumping well is very small so that storage in the well can be neglected

Hantush and Jacob (1955, 1961a and b) developed a well function that accounts for confining layer leakage and it is one of the most common solutions used to analyze leaky aquifers. Walton (1991) gives the equation for drawdown in a leaky confined aquifer as:

$$s = \frac{Q}{4\pi T} W\left(u, \frac{r}{B}\right) \quad (2-8)$$

where Q is the extraction flow rate, T is the transmissivity. $W(u, r/B)$ is the Hantush-Jacob leaky well function defined by:

$$W\left(u, \frac{r}{B}\right) = \int_u^{\infty} \frac{1}{y} e^{\left\{-y - \frac{(r/B)^2}{4y}\right\}} dy \quad (2-9)$$

where u is defined by Equation 2-5 and:

$$\frac{r}{B} = \frac{r}{\sqrt{\left(\frac{Tb'}{k'}\right)}} \quad (2-10)$$

where r is the radial distance from the pumping well, B is the leakage factor, T is transmissivity, b' is the confining layer thickness, and k' is the permeability of the confining layer. The assumptions of the Hantush-Jacob solution are the same as those for the Theis solution except for leakage from the confining layer.

Transmissivity is converted to hydraulic conductivity with following equation:

$$K = \frac{T}{b} \quad (2-11)$$

where K is hydraulic conductivity, T is transmissivity, and b is aquifer thickness.

The Hantush-Jacob method was implemented using a computer code named AQTESOLV (Duffield, 2007). Parameters used in the Hantush-Jacob model for leaky aquifers include the saturated thickness of the aquifer, the thickness of the overlying confining layer, and the zone of penetration of the pumping and observation wells. The hydrogeologic conceptual model described in Section 2.2 was used to establish the layer thicknesses used in AQTESOLV.

Derivative analysis was used to aid in interpretation of the pumping test data. Derivative analysis is useful for identifying flow regimes, wellbore storage effects, and selecting appropriate aquifer models. AQTESOLV was used to conduct the derivative analysis of the drawdown data. Derivative plots were created by plotting the derivative of the drawdown type curve as a function of time on a log axis. These plots were compared to standard plots in the AQTESOLV library to identify flow regime and aquifer type.

2.6 Barometric Effects

Fluctuations in barometric pressure can impact water level measurements in a confined aquifer even when vented pressure transducers are used because the well serves as a direct connection to the atmosphere for the aquifer. Any change in atmospheric pressure is immediately transmitted to the aquifer through the opening provided by the well screen. For wells near the pumping well, barometric effects may be minimal in comparison to the head change induced by pumping. However, for wells further away where the head change in the aquifer is smaller, barometric effects can be significant. Data collected during the constant rate aquifer testing at RWM019 were corrected for barometric effects.

Corrections to water level data were made using the following equations (Gonthier, 2007).

$$\Delta w_{cor} = w_{obs} - B_{eff} * \Delta BP \quad (2-12)$$

where w_{cor} = corrected water level, ft H₂O

w_{obs} = observed water level, ft H₂O

B_{eff} = Barometric efficiency

ΔBP = change in barometric pressure, ft H₂O

$$B_{eff} = \frac{\Delta wl}{\Delta BP} \quad (2-13)$$

where B_{eff} = Barometric efficiency

Δwl = change in water level, ft H₂O

ΔBP = change in barometric pressure, ft H₂O

Water level measurements were made in the observation wells prior to the RWM019 aquifer test to establish baseline hydraulic conditions. These data were used to calculate the barometric efficiency of each well which was then used to correct the water level measurements collected during the constant rate aquifer test.

3.0 Results

Well performance and aquifer testing were conducted at RWM019. The test methods employed are described in Section 2.0. Pretest monitoring began at most observation wells on or around July 14, 2020. Step-drawdown testing began at RWM019 on July 30, 2020 and was completed the same day. The constant rate aquifer test began on August 12, 2020 and active monitoring of water levels continued through September 14, 2020. The constant rate aquifer test consisted of a 21-day pumping period and a 12-day recovery period. Testing was conducted with the other wells in the recovery network operating at near steady-state conditions so that any observed aquifer response could be attributed to testing at RWM019. The following sections provide a discussion and analysis of the results obtained from the hydrologic testing.

3.1 Barometric Efficiency

Prior to the RWM019 aquifer pumping test, water level measurements were recorded for several weeks to evaluate the effects of barometric pressure. Barometric efficiencies were calculated for

each observation well (except MSB003BR) using the methods described in Section 2.6 and are presented in Table 3. Values ranged from 31 to 74% with a median of 57% (average 56%). The median barometric correction for the observation monitoring wells was about 0.05 ft. A barometric efficiency was not calculated for MSB003BR because the resolution of the transducer used in this well was on the same order as the measured barometric fluctuations.

With the exception of MSB003BR, the median efficiency (57%) was used to correct water level data prior to analysis using the methods outlined in Section 2.6. Figure 6 and Figure 7 show a subset of the hydrologic data collected for wells MSB 14A and MSB 14B. The effects of barometric pressure changes are evident as uncorrected water levels trend inversely with barometric pressure. These plots also show the effectiveness of the corrections made to the data as the corrected water levels show negligible correlation to barometric pressure.

3.2 Step Drawdown Testing

A step-drawdown test was conducted on RWM019 on 7/30/2020 to determine well performance characteristics. The test consisted of three steps lasting approximately 120 minutes each with pumping rates of 49, 64, and 79 gpm. Due to an obstruction in RWM019 (~140 ft bgs), it was not possible to insert a pressure transducer to monitor the response to the step-test. Therefore, water levels in RWM019 were manually recorded during the test using a water level tape. Flow rates were also manually recorded. Data recorded from RWM019 during the step-drawdown test are presented in Figure 8.

Due to the short duration of the step-drawdown test and the magnitude of drawdown observed in the pumping well, it was unnecessary to make corrections for barometric effects. The total drawdown observed in RWM019 was 30.4 ft, whereas the maximum barometric fluctuation recorded over the duration of the test was less than 0.1 ft.

The specific capacity of RWM019 was calculated at the end of each pumping interval (Table 4). Based on the results of the step-drawdown test, the specific capacity of RWM019 was determined to be 2.62 gpm/ft (estimated from final step). Specific discharge (inverse of specific capacity) was determined for each pumping period and plotted as a function of pumping rate (Figure 9). The slope and intercept of this plot were used to estimate the Jacob (1947) head loss coefficients, B

and C. The aquifer head loss coefficient (B) was determined to be 2.3 ft/ft³/min and the well loss coefficient (C) was determined to be 0.05 min²/ft⁵ (Table 5).

Well efficiency was calculated for each pumping period and plotted as a function of pumping rate (Figure 10). The efficiency of RWM019 at the end of the final pumping period was estimated to be 81%. The head loss coefficients were used to predict drawdown at the end of each pumping period for the step-drawdown test (Figure 11). Good agreement is noted between the predicted and observed drawdown.

The head loss coefficients, B and C, were also used to calculate drawdown as function of pumping rate (Figure 11). Figure 12 provides a plot of predicted drawdown in RWM019 as a function of pumping rate along with the screened interval and pump placement. Under the maximum operating conditions (~79 gpm), the water level in RWM019 is estimated to be 8.6 ft above the pump.

Aquifer response to the step-drawdown testing was monitored in the wells identified in Table 2. The maximum drawdown observed in each well over the course of the short duration test is presented in Table 6. A response was measured at each observation well except for MSB003BR and SSM029B. The pressure transducer installed at MSB003BR did not have adequate resolution to measure the response due to the step-drawdown test. SSM29B is the most distant observation well for the RWM019 aquifer testing (1930 ft). Therefore, this well was not expected to have a discernable response during the short duration step-drawdown testing. In general, the measured drawdown values (Table 6) during the step-drawdown test were less than those estimated for steady-state conditions (Table 2). This is attributed to the short duration of the step-drawdown test (~6 hours) which was not long enough for water levels to reach steady state.

3.3 RWM019 Aquifer Test

Following the step-drawdown test, the aquifer was allowed to recover to near pre-test conditions. The RWM019 constant rate aquifer pumping test commenced on August 12th, 2020 at 09:00 AM and continued through September 2nd, 2020 at 09:00 AM for a period of 21 days. Post-test monitoring of recovery in the observation wells continued until September 14th, 2020. The average and median flow rates were 79.1 gpm for the 21-day test period ($\sigma = 0.2$ gpm). The flow from RWM019 was nearly constant during the pumping period (Figure 23). Drawdown data for each

observation well are presented in Figure 24 through Figure 38. Maximum corrected drawdown is presented in Table 7. Following pumping, aquifer recovery was monitored from September 2nd, 2020 through September 12th, 2020 for a total of 10 days.

The recovery well network was maintained at steady state prior to and during the constant rate pumping test. With the exception of RWM 1, all wells operated at near steady flow conditions (Table 8). RWM 1, which typically operates at a flow rate of about 10 gpm and is screened in the upper portion of the aquifer, shutdown unexpectedly three times in the later portion of the pumping test [elapsed time >20,000 mins] (Table 9). After repairs were made, RWM 1 operated continuously for the remainder of the test. The effect of these brief shutdown periods is most noticeable in the drawdown data for MSB003CR (Figure 31) and to a lesser extent at MSB004CR (Figure 34). These wells are the closest to RWM 1 and are screened in the upper part of the aquifer as is RWM 1. Drawdown observed in both wells decreased during the shutdown periods as stress from pumping at RWM 1 was removed from the aquifer.

Perturbations in drawdown were noticeable in several other observation wells that were not attributable to the interruptions at RWM 1. For example, the drawdown data for MSB004BR shows several perturbations prior to the RWM 1 shutdowns (Figure 32). In the early portion of the test (0-5,000 mins), there are two noticeable periods where drawdown decreased. Likewise, in the middle portion of the test (15,000 to 20,000 mins), fluctuations in drawdown were observed. These fluctuations may be due to flow variations at RWM 10. Since flowrate was not logged at RWM 10, it is not possible to conclusively identify the source of the fluctuations.

Perturbations in drawdown were also noticed in several wells at elapsed times of approximately 2,500; 4,900; and 17,500 minutes. These perturbations were more noticeable in wells farther from RWM019 and the recovery well network in general (e.g. MSB 39B, MSB 63B, and SSM029B). SSM029B is the most distant observation well from RWM019 (1930 ft) used in the aquifer testing. The effect of RWM019 pumping and recovery are clear in the drawdown data for SSM029B as well as the influence from an unidentified source (Figure 38). After reviewing nearby pumping wells (including PW 20A and PW 53A), the source of these perturbations in aquifer pressure could not be identified.

3.4 Analysis of LLAZ Hydraulic Properties

Aquifer response due to pumping at RWM019 was monitored during the step-drawdown testing and during the constant rate aquifer test that followed. Datasets from both tests were analyzed to estimate the hydraulic properties of the LLAZ near RWM019 using AQTESOLV (Duffield, 2007). The hydrogeologic conceptual model presented in Section 2.2 was used to establish boundaries and dimensions for the analysis (Table 10). The Hantush-Jacob (1955, 1961a and b) leaky, confined model was chosen for the analysis as discussed in Section 2.5. An aquifer thickness of 60 ft was used for all analyses except for MSB 39B and MSB 63B which are screened near the bottom of the aquifer (Figure 4). For these two wells, an aquifer thickness of 65 ft was used to accommodate the deeper screens. An aquitard thickness of 4 ft was used in all analyses.

Data for all testing was collected on 1-minute intervals. A high sampling rate was selected due to the unpredictable operating conditions for the recovery well network. This resulted in the collection of thousands of data points for each observation well. As such, each data set was filtered using AQTESOLV to improve computational efficiency and, to improve the quality of fit to the observed data. Pumping rates were collected on the same frequency during the constant rate test and were also filtered.

3.4.1 Analysis of Step-Drawdown Test Data

Pressure data measured in each observation well during the step-drawdown test was analyzed to determine aquifer hydraulic properties. The results of these analyses are presented in Table 11 and Figure 13 through Figure 22. Transmissivity values ranged from 0.96 to 3.2 ft²/min with an average value of 2.1 ft²/min ($\sigma = 0.71$ ft²/min). Transmissivity was converted to hydraulic conductivity using Equation 2-10. Hydraulic conductivity ranged from 23 to 76.1 ft/day with an average value of 48.7 ft/day. Storativity values ranged from 0.0001 to 0.0009 with an average value of 0.0005 ($\sigma = 0.0002$). Leakage values (r/B) ranged from 0.0000 to 0.6749 with an average value of 0.2470 ($\sigma = 0.2543$). Equation (2-11) was solved for K' which is the hydraulic conductivity of the overlying confining layer (GCCZ). Values for K' ranged from 0.000 to 0.005 ft/day with an average value of 0.002 ft/ day.

3.4.2 Analysis of Constant Rate Aquifer Test Data

During the constant rate aquifer test, the recovery well network operated at near steady state conditions except for RWM 1. RWM 1 shutdown unexpectedly three times during the constant rate aquifer test (Table 9). The effect of these shutdowns on aquifer pressure was seen in the drawdown data from several nearby observation wells. The short duration, unplanned shutdowns at RWM 1 complicated analysis of the constant rate aquifer test because flow rates were only logged at RWM019.

The influence of the shutdowns on drawdown made it necessary to account for RWM 1 in the AQTESOLV model for the constant rate pumping test. To minimize uncertainty associated with flow from RWM 1, it was treated as an injection well (as opposed to an extraction well) with a flow rate of zero when the well was pumping and a flow rate of -9 gpm during shutdown periods (Table 8). The timing of the shutdown periods was inferred from the drawdown data obtained from nearby observation wells and from ACP round sheets.

Accounting for RWM 1 in the AQTESOLV model improved the quality of fit to the drawdown data, particularly for observation wells near RWM 1. Since the other recovery wells in the network operated at near steady flow conditions prior to and during the constant rate test, it was not necessary to include them in the AQTESOLV model.

Pressure data from both the pumping and recovery periods were analyzed together using AQTESOLV. Data from each well was analyzed independently to determine aquifer hydraulic properties. Drawdown and recovery data were analyzed together. Estimates of transmissivity, storativity, and leakage were obtained from the analysis. Hydraulic conductivity of both the LLAZ and the overlying confining layer (GCCZ) was calculated from the AQTESOLV output. The results of the analyses are presented Table 12 and Figure 40 through Figure 51.

Transmissivity values ranged from 0.55 to 3.30 ft²/min with an average value of 1.70 ft²/min (σ = 0.76 ft²/min). Hydraulic conductivity ranged from 13.2 to 73.1 ft/day with an average value of 39.9 ft/day. Storativity values ranged from 0.0002 to 0.006 with an average value of 0.0014 (σ = 0.0016). Leakage values (r/B) ranged from 0.0195 to 0.7570 with an average value of 0.1874 (σ = 0.2603). The hydraulic conductivity of the overlying confining layer (GCCZ), K', ranged from 0.0000 to 0.0036 ft/day with an average value of 0.0001 ft/ day.

Derivative analysis was used to identify the flow regime and aquifer type based on the results of the constant rate aquifer test. The derivative of the drawdown type curve for each observation well is presented in Figure 40 through Figure 51. The shape of the derivative curve for each well is consistent with a leaky, confined aquifer with infinitely acting radial flow (Duffield, 2007). At the end of the constant rate aquifer pumping test, the specific capacity of RWM019 was estimated to be 2.3 gpm/ft.

3.4.3 Analysis of Aquifer Response to RWM 1

Although the unplanned shutdowns of RWM 1 complicated the analysis of the RWM019 constant pumping rate aquifer data, they also provided an opportunity to analyze aquifer properties based on the observed pressure response due to RWM 1. Figure 31 and Figure 34 show that drawdown measured at MSB003CR and MSB004CR was near steady state when RWM 1 shutdown. This allowed for the aquifer response in these two wells during the shutdown periods to be assigned to RWM 1. Therefore, data from the second RWM 1 shutdown period (Table 9) for MSB003CR and MSB004CR were extracted and analyzed separately to estimate aquifer properties. For this analysis, the pumping well was RWM 1 and the pumping rate was 10 gpm. Other extraction wells were excluded from the analysis because they were operating at near steady state conditions.

The shutdown of RWM 1 produced a pressure decline in both wells as stress was removed from the aquifer due to pumping. This decline was converted to drawdown for this analysis. The second shutdown of RWM 1 produced a maximum drawdown of 0.28 ft in MSB003CR and 0.12 ft in MSB004CR. AQTESOLV was used to analyze the drawdown data using the same aquifer dimensions as used for the RWM019 dataset. Although RWM 1 is partially screened in the LLAZ, for simplicity it was treated as a fully penetrating well. This simplification is reasonable since MSB003CR and MSB004CR are a distance from the pumping well greater than 1.5 times the aquifer thickness (Kruseman and de Ridder, 1994). For the purpose of this analysis, it was assumed that all flow was derived from the LLAZ.

The results of the analyses are shown in Figure 53 and Figure 54 for MSB003CR and MSB004CR. The transmissivity estimated for MSB003CR was 1.37 ft²/min compared to 1.34 ft²/min from the RWM019 dataset. The transmissivity estimated for MSB004CR was 2.06 ft²/min compared to 1.75 ft²/min from the RWM019 dataset.

3.4.4 Summary of Hydraulic Properties

Best estimate aquifer properties were determined by averaging the results from the step-drawdown test and the constant rate aquifer pumping test (Table 13). The average transmissivity of the aquifer based on all testing was determined to be 1.87 ft²/min with a standard deviation of 0.74 ft²/min. The average storativity of the aquifer was determined to be 0.001 with a standard deviation of 0.0012. The average hydraulic conductivity of the LLAZ near RWM019 was determined to be 43.9 ft/day with a standard deviation of 16.8 ft/day, which is comparable to a clean sand (Freeze and Cherry, 1979). The average hydraulic conductivity of the overlying confining layer (GCCZ), K', was determined to be 0.002 ft/day with a standard deviation of 0.0024 ft/ day, which is indicative of silt/clay (Freeze and Cherry, 1979).

3.5 Verification Calculations

A verification calculation was performed using data from the RWM019 aquifer pumping test for MSB 14A. A spreadsheet calculation was made using the equations provided in Section 2.5 to estimate transmissivity and storativity using the Theis confined aquifer solution. Figure 56 shows a plot of the observed and predicted drawdown for MSB 14A (Theis method). The transmissivity (1.88 ft²/min) and storativity (0.0001) values from this analysis were comparable to values determined using AQTESOLV and the Theis solution (1.64 ft²/min and 0.0001). The transmissivity values calculated with the Theis solution are slightly larger than those determined with the Hantush-Jacob leaky aquifer method for MSB 14A (Table 12). The Theis model, which does not account for confining layer leakage, assumes all water comes from storage in the pumped aquifer. For leaky aquifers, this results in higher estimates of aquifer transmissivity compared to the Hantush-Jacob model.

As an additional check of the aquifer property estimates, median property values from the constant rate pumping test were used to calculate drawdown for the observation wells used in the RWM019 constant rate aquifer test. The verification calculation was made using Excel and the Solver feature. Additionally, the most recent version of the A/M area groundwater flow model was used to simulate drawdown (SRNS, 2017). All properties were left unchanged in the groundwater model except the pumping rate for RWM019 which was increased from 50 to 75 gpm. Figure 57 presents a comparison of the measured and predicted drawdown values. The measured drawdown in RWM019 exceeded the calculated and model simulated drawdown. Neither the calculated nor the

model simulated drawdown estimates account for well losses which may partially explain the noted differences. The well efficiencies determined using the calculated and model simulated drawdown values are 44% and 54%. These values are lower than estimated from the step drawdown testing (81%, Section 3.2).

Drawdown predicted with the median aquifer properties compared better to the measured drawdown than the model simulated drawdown. In the area of RWM019, the model uses a hydraulic conductivity of 10 ft/day which is equivalent to a transmissivity of 0.42 ft²/min. The median aquifer transmissivity from the constant pumping rate test was 1.36 ft²/min (Table 12). The lower transmissivity used in the model results in larger drawdown values, particularly close to the pumping well as shown in Figure 57.

4.0 Conclusions

An aquifer pumping test was conducted on the LLAZ at the recently installed recovery well RWM019 in accordance with the approved test plan (Dixon, 2020). The objective of the testing was to determine baseline well performance parameters and aquifer hydraulic conductivity. This testing consisted of a step-drawdown test to determine well performance properties, a constant pumping rate aquifer test to determine aquifer hydraulic properties, and a post-test aquifer recovery monitoring period also used to estimate aquifer hydraulic properties. Well performance parameters determined included specific capacity, well efficiency, and head loss coefficients. The specific capacity of RWM019 was determined to be approximately 2.6 gpm/ft of drawdown based on the final step of the step-drawdown test. Well efficiency was inversely related to pumping rate and decreased from 87% to 81% over a pumping range of approximately 49 to 79 gpm. The aquifer head loss coefficient was determined to be 2.3 ft/ft³/min and the well loss coefficient was determined to be 0.05 min²/ft⁵.

Aquifer response to pumping at RWM019 was measured in several nearby observation wells screened within the LLAZ. Drawdown data were collected during the step-drawdown test and during the constant rate pumping test. Recovery data were also collected following shutdown of RWM019. These data were used to evaluate aquifer hydraulic properties using the Hantush-Jacob (1955, 1961a, and b) leaky aquifer model as implemented in the computer code AQTESOLV (Table ES1). The average transmissivity (T) of the aquifer based on all testing was determined to

be 1.87 ft²/min with a standard deviation of 0.74 ft²/min. The average storativity of the aquifer was determined to be 0.001 with a standard deviation of 0.0012. The average hydraulic conductivity of the LLAZ near RWM019 was determined to be 43.9 ft/day with a standard deviation of 16.8 ft/day. The average hydraulic conductivity of the overlying confining layer (GCCZ), K', was determined to be 0.002 ft/day with a standard deviation of 0.0024 ft/ day.

At the time the original recovery well network was installed, extensive hydraulic testing was conducted to determine aquifer hydraulic properties. Of the recovery wells in the original network, RWM 7 and RWM 10 are the closest to RWM019. The transmissivity of the aquifer at RWM 7 and RWM 10 was reported as 1.95 and 2.32 ft²/min, respectively (Geraghty and Miller. 1987). The results from the testing of RWM019 are comparable to the previous testing and suggest the aquifer is more transmissive in this area than near RWM018 where a transmissivity of 0.816 ft²/min was measured (Dixon, 2018).

5.0 References

Dixon, K. L. 2020. Hydraulic Testing of Recovery Well RWM019. SRNL-RP-2020-00149, Savannah River National Laboratory, Aiken, SC.

Dixon, K. L. 2019. Hydraulic Testing of the Lost Lake Aquifer Near Recovery Well RWM 8. SRNL-STI-2019-00476. Savannah River National Laboratory, Aiken, SC.

Dixon, K. L. 2018. Hydraulic Testing of Lost Lake Aquifer Near Recovery Wells RWM018, RWM 3, and RWM 5. SRNL-STI-2018-00434. Savannah River National Laboratory, Aiken, SC.

Fetter, C. W. 1994. Applied Hydrology, 3rd edition. Prentice-Hall, Inc. London, UK.

Freeze, R. A. and J. A. Cherry. 1979. Groundwater. Prentice-Hall, Inc. Englewood Cliffs, NJ.

Duffield, G. M. 2007. AQTESOLV Pro for Windows Version 4.5. HydroSOLVE, Reston, VA 20191. <http://www.aqtesolv.com/>.

Geraghty and Miller. 1987. Evaluation of Recovery-Well Efficiency, Specific Capacity, and Transmissivity Estimation. Prepared for E. I. du Pont de Nemours & Co., Inc., Savannah River Plant, Aiken SC.

Gonthier, G. J. 2007. A Graphical Method for Estimating Barometric Efficiency from Continuous Data – Concepts and Applications to a Site in the Piedmont, Air Force Plant 6, Marietta, Georgia: U. S Geological Survey Scientific Investigations Report 2007-5111 (<http://pubs.usgs.gov>).

Hantush, M. S. and C. E. Jacob, 1955. Non-steady radial flow in an infinite leaky aquifer. American Geophysical Union Transactions. Vol. 36, pp. 95-100.

Hantush, M. S. 1961a. Drawdown around a partially penetrating well. Journal of the Hydraulics Division, Proceedings of the American Society of Civil Engineers. Vol. 87, No. HY4, pp. 83-98.

Hantush, M. S. 1961b. Aquifer tests on partially penetrating wells. Journal of the Hydraulics Division, Proceedings of the American Society of Civil Engineers. Vol. 87, No. HY5, pp. 171-194.

Hiergesell, R. A. 1992. Hydrologic Analysis of Data for the Lost Lake Aquifer Zone of the Steed Pond Aquifer at Recovery Well RWM 16. WSRC-TR-92-529. Westinghouse Savannah River Company, Aiken, SC.

Jacob, C. E. 1947. Drawdown Test to Determine the Effective Radius of An Artesian Well. Transactions of the ASCE, Vol. 112, pp. 1047-1070.

Kruseman G. P. and N. A. de Ridder. 1994. Analysis and Evaluation of Pumping Test Data. 2nd Edition. International Institute for Land Reclamation and Improvement, Wageningen, The Netherlands.

Marine, I. W. and H. W. Bledsoe. 1984. Supplemental Technical Data Summary, M-Area Groundwater Investigation. DPSTP-84-112. Savannah River Laboratory, E. I. Dupont de Nemours Co., Aiken, SC.

SRNS, 2017. Capture Zone Analysis for Various Recovery Well Scenarios, M-1 Air Stripper System (U). A/M Area Groundwater Operable Unit. ERD-EN-2017-0041. Savannah River Nuclear Solutions, Aiken, SC.

Theis, C.V., 1935. The relation between the lowering of the piezometric surface and the rate and duration of discharge of a well using groundwater storage. American Geophysical Union Transactions, Vol. 16, pp. 519-524.

Walton, W. C. (1991). Principles of Groundwater Engineering. Lewis Publishers Inc., Chelsea, MI.

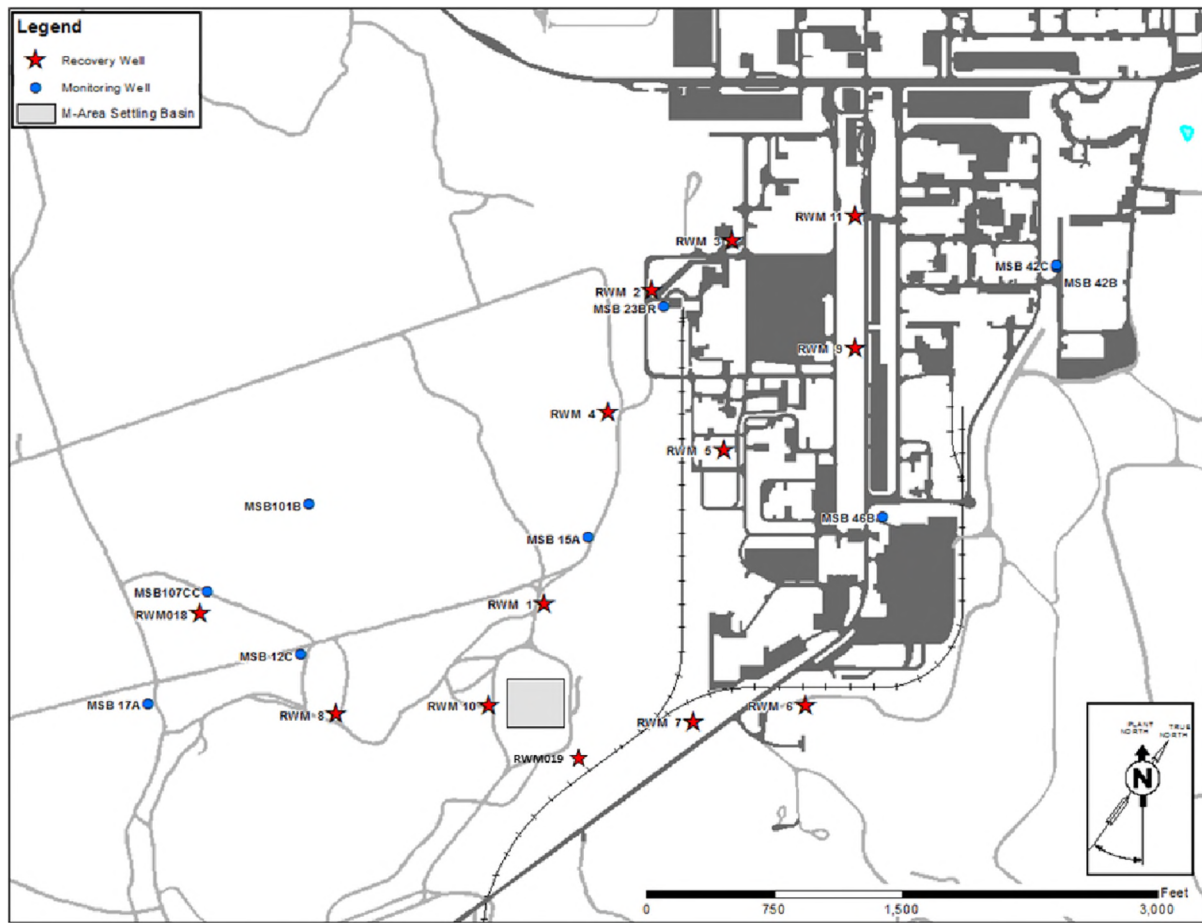


Figure 1. Location of Recovery Wells.

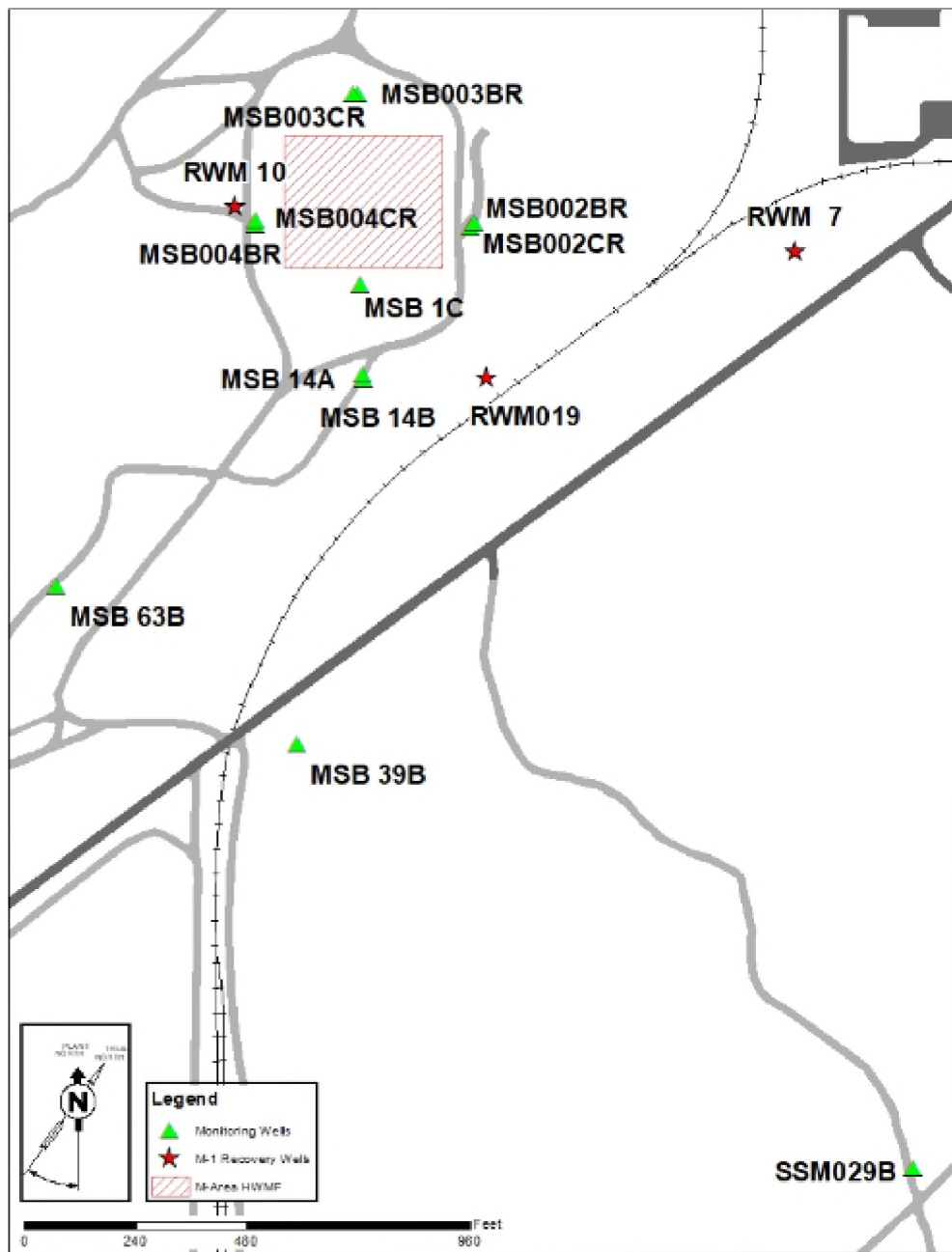


Figure 2. Location of Recovery Well RWM019 and Nearby Monitoring Wells.

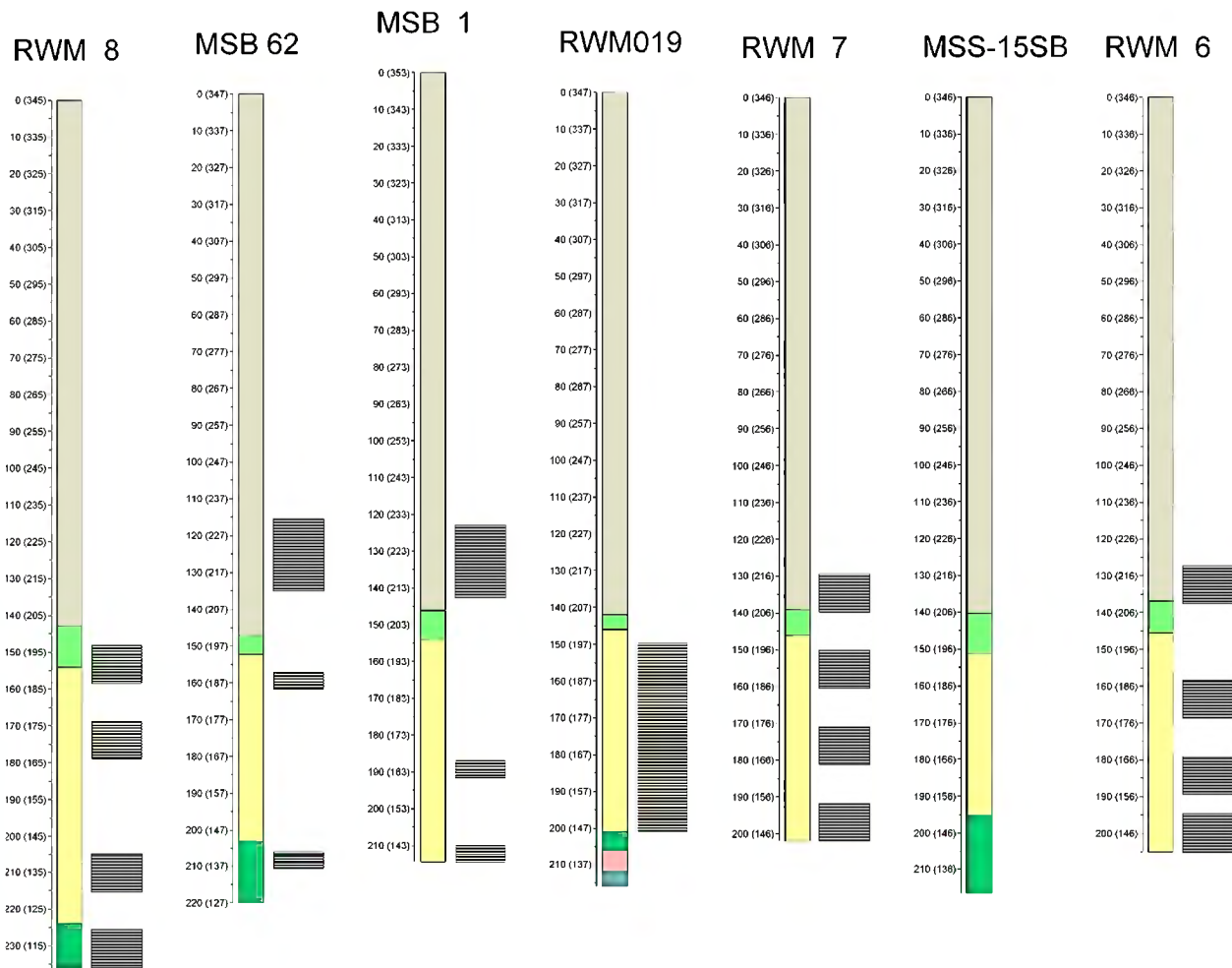


Figure 3: Generalized Lithologic Cross Section Near RWM019.

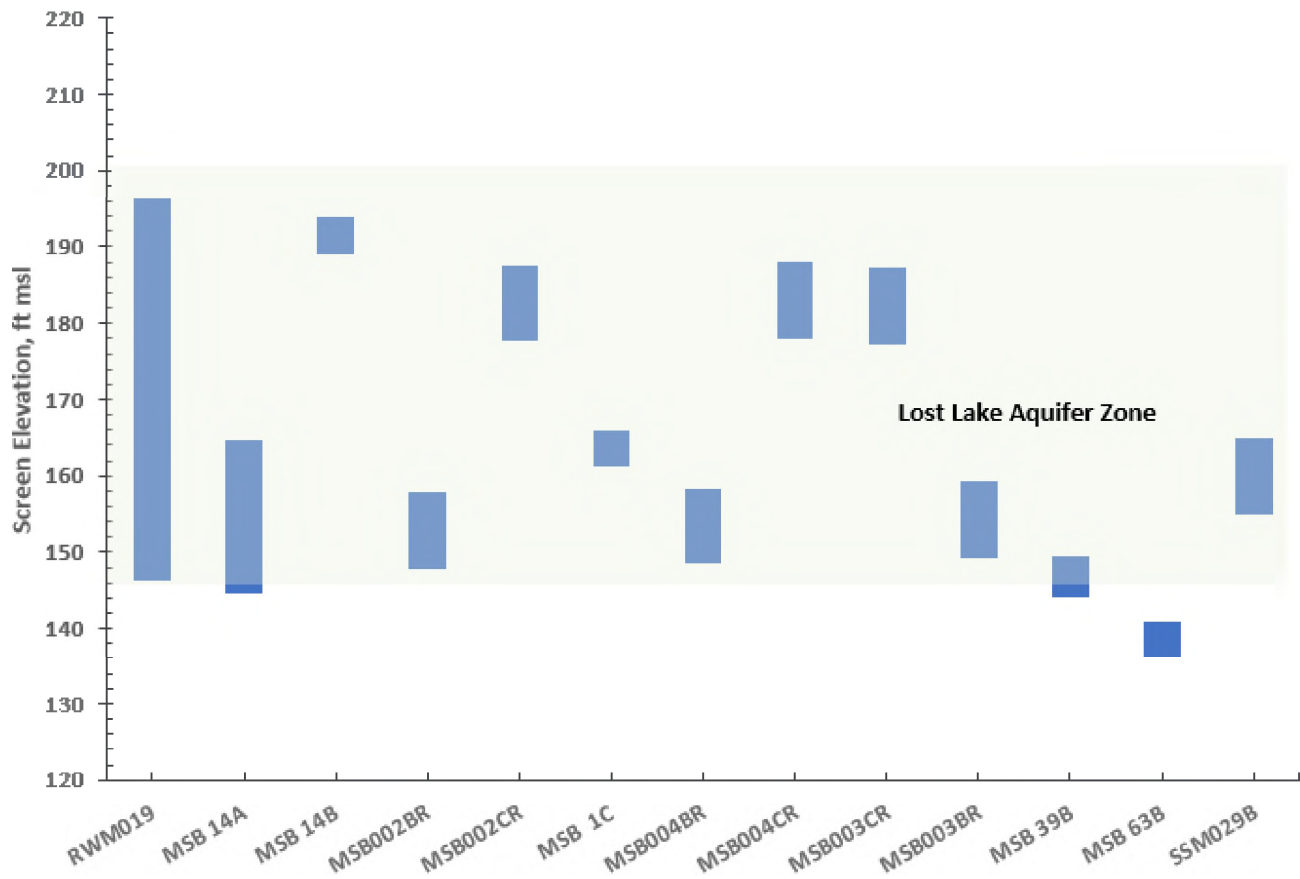


Figure 4. Screen Elevations for RWM019 Aquifer Test Wells.

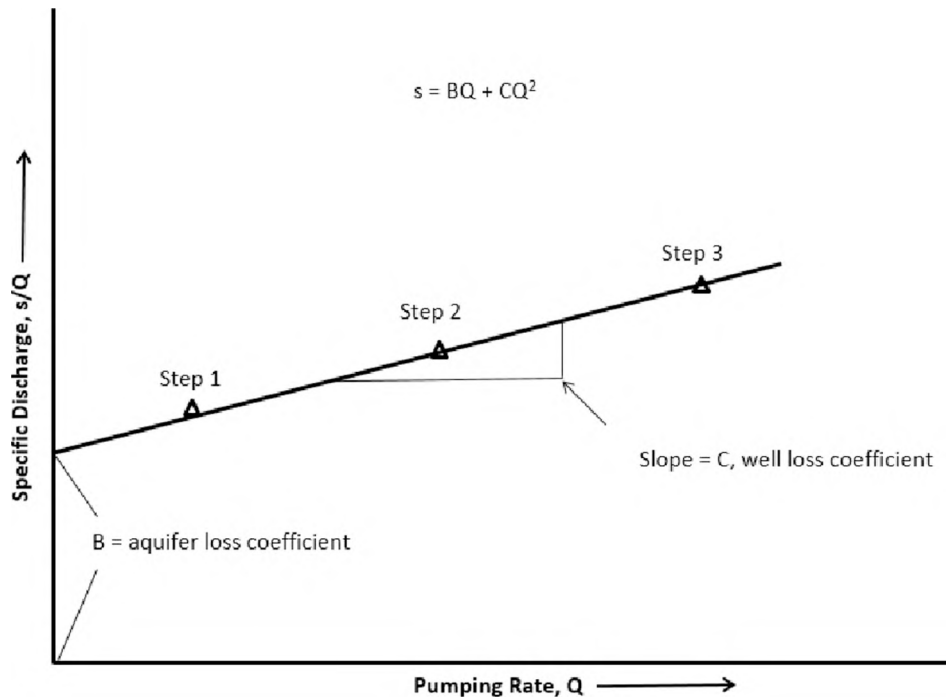


Figure 5: Plot for Calculating Formation Loss Coefficient B and Well Lose Coefficient C from Step Drawdown Tests (adapted from Spane and Newcomer, 2007).

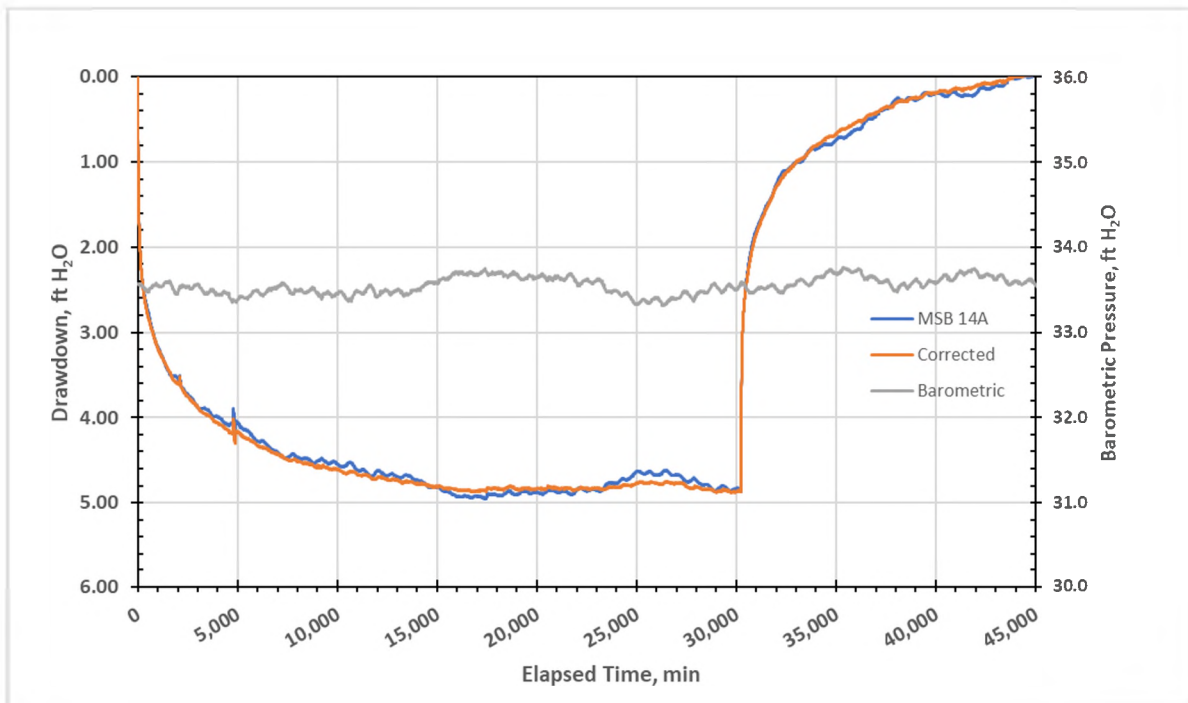


Figure 6: Effect of Barometric Efficiency Corrections to Water Level Data from MSB 14A.

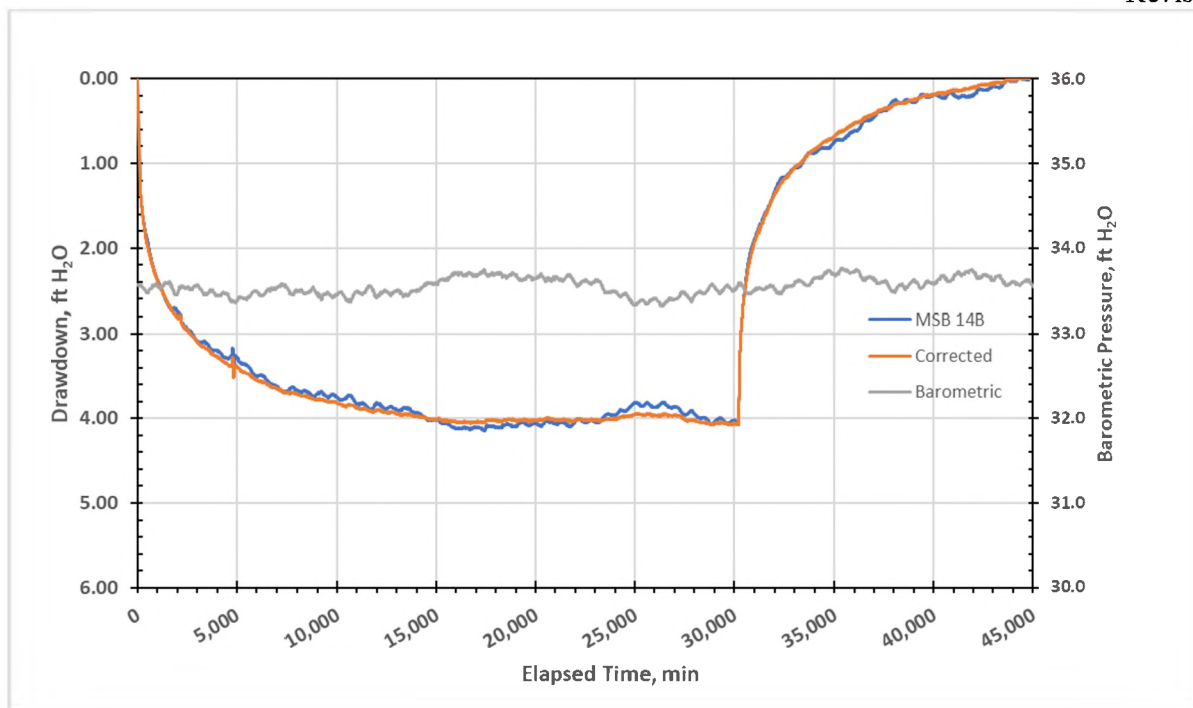


Figure 7: Effect of Barometric Efficiency Corrections to Water Level Data from MSB 14B.

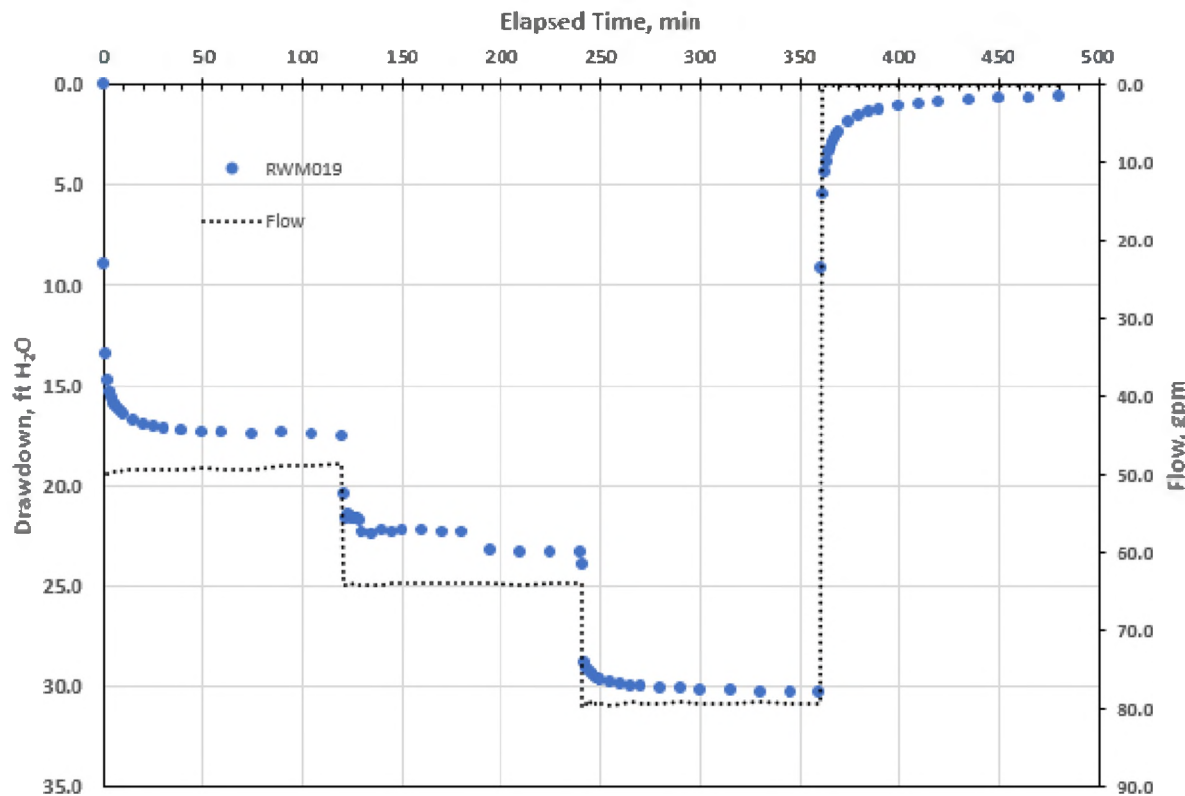


Figure 8. Drawdown as a Function of Time for RWM019 Step Test.

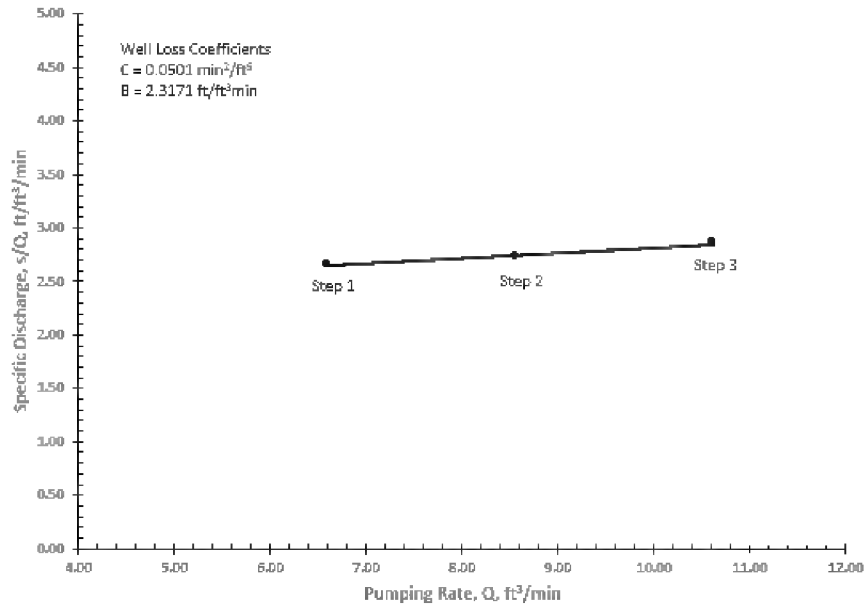


Figure 9. Specific Discharge as a Function of Pumping Rate for RWM019.

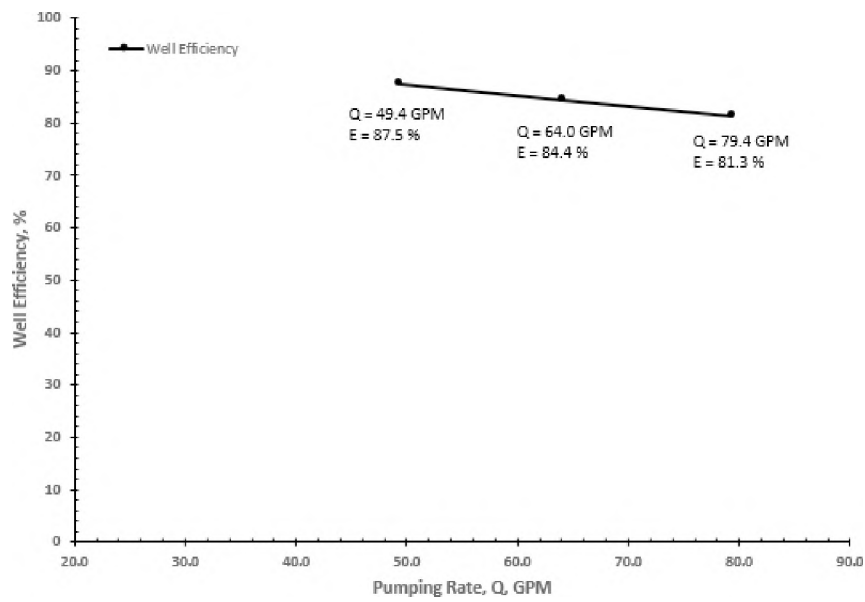


Figure 10. Well Efficiency as a Function of Pumping Rate for RWM019.

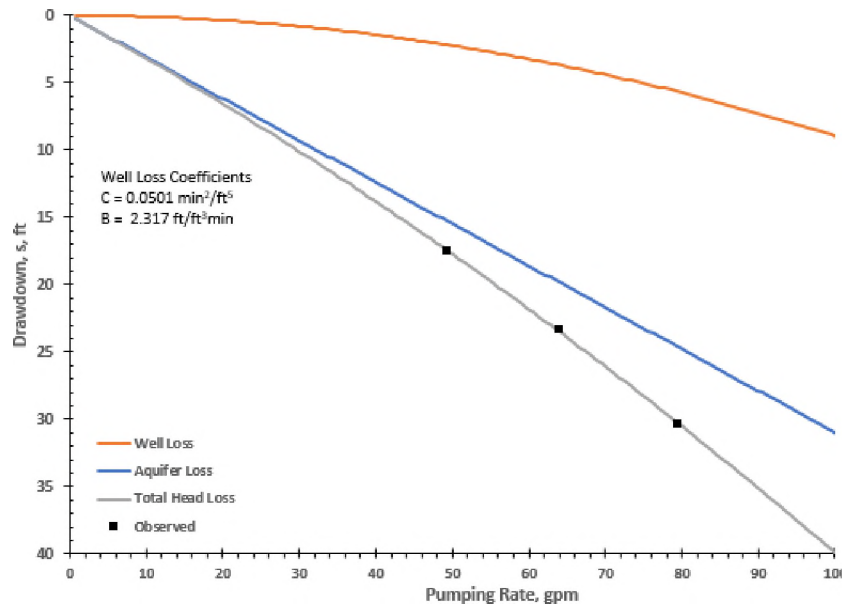


Figure 11. Head Loss Plot for Step-Drawdown Test at RWM019.

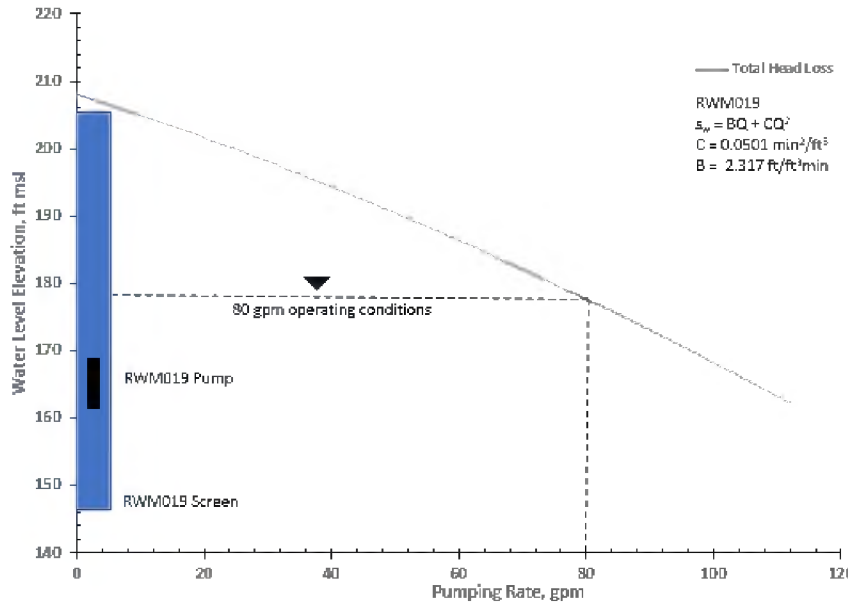


Figure 12. Head Loss Plot for RWM019.

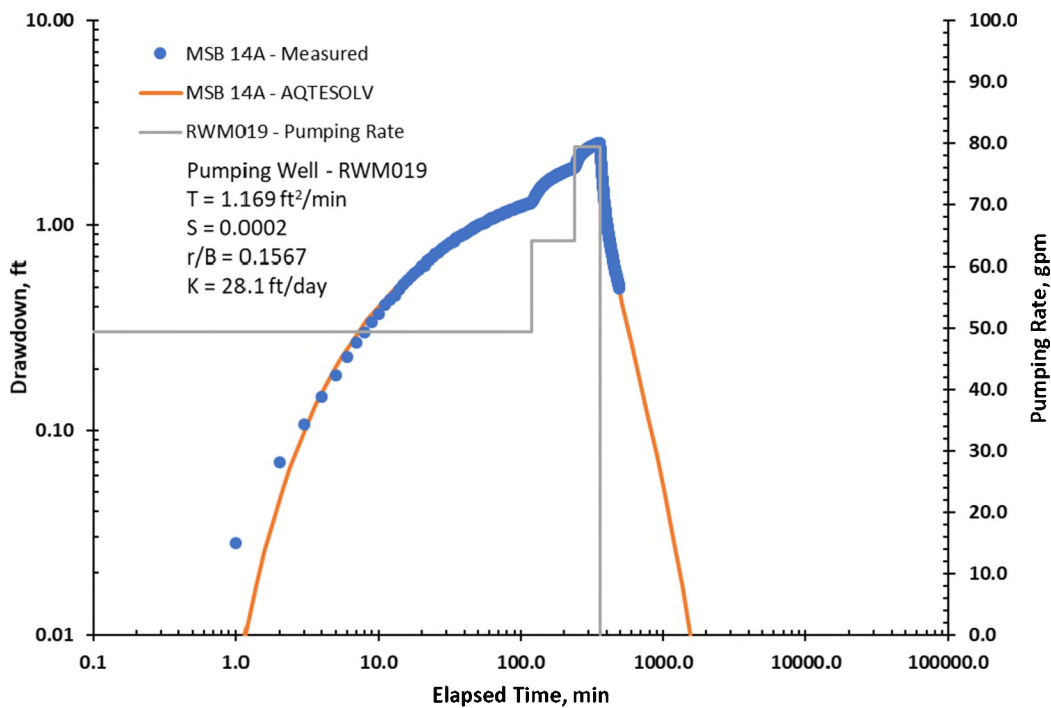


Figure 13. Step Test Drawdown Data and Hantush-Jacob Leaky Aquifer Type Curve for MSB 14A.

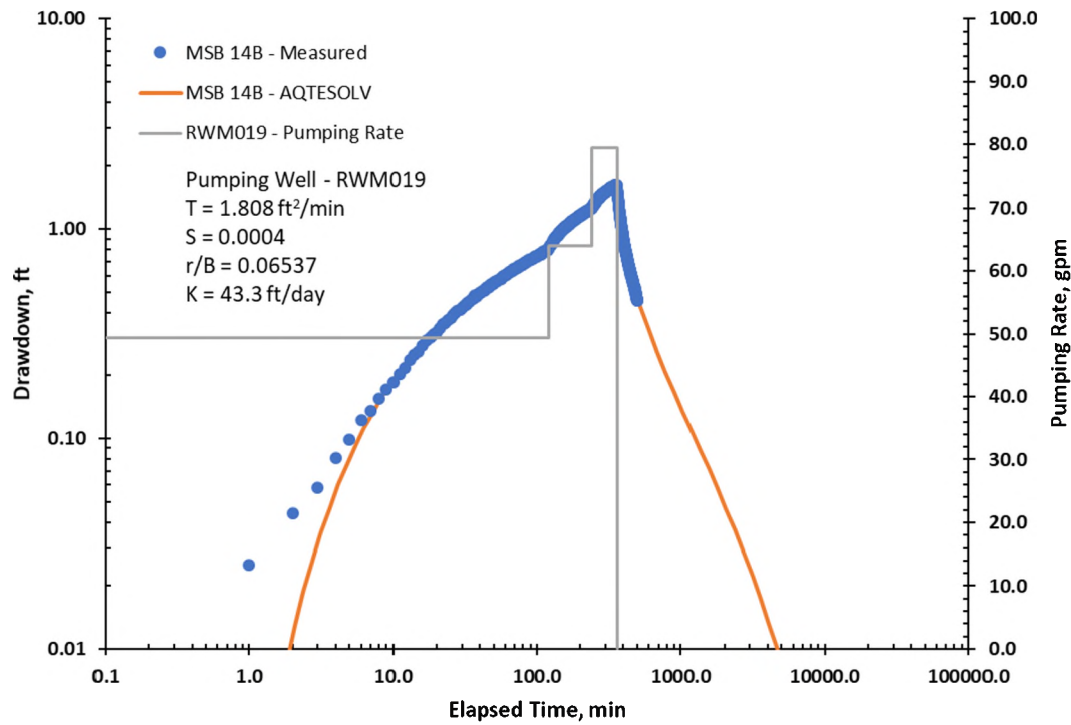


Figure 14. Step Test Drawdown Data and Hantush-Jacob Leaky Aquifer Type Curve for MSB 14B.

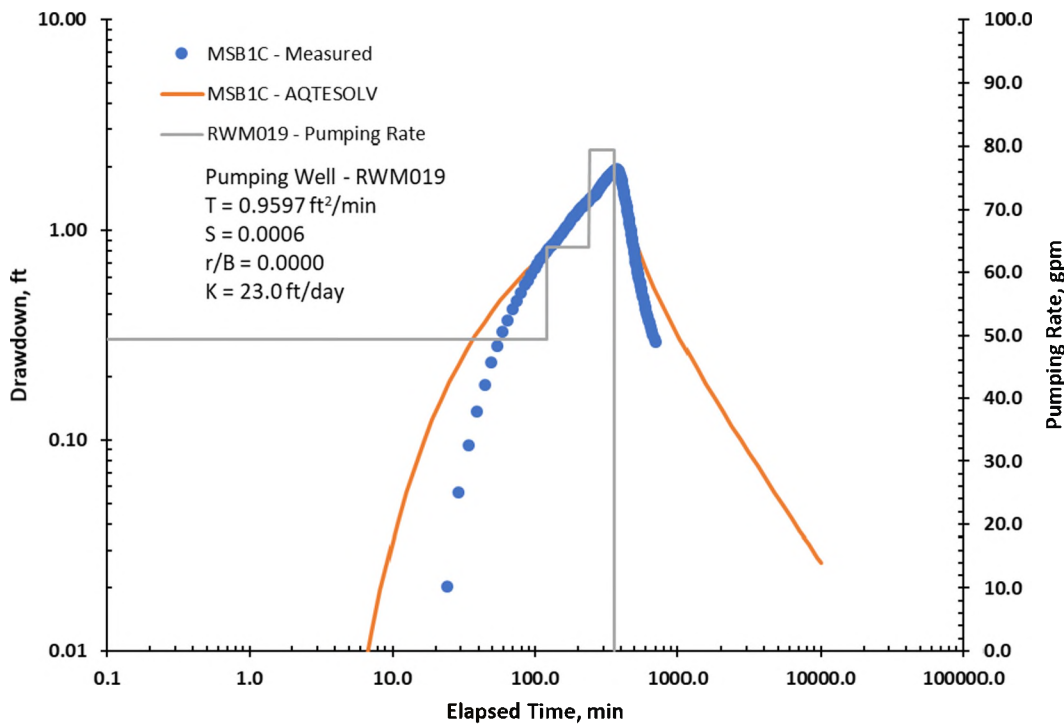


Figure 15. Step Test Drawdown Data and Hantush-Jacob Leaky Aquifer Type Curve for MSB 1C.

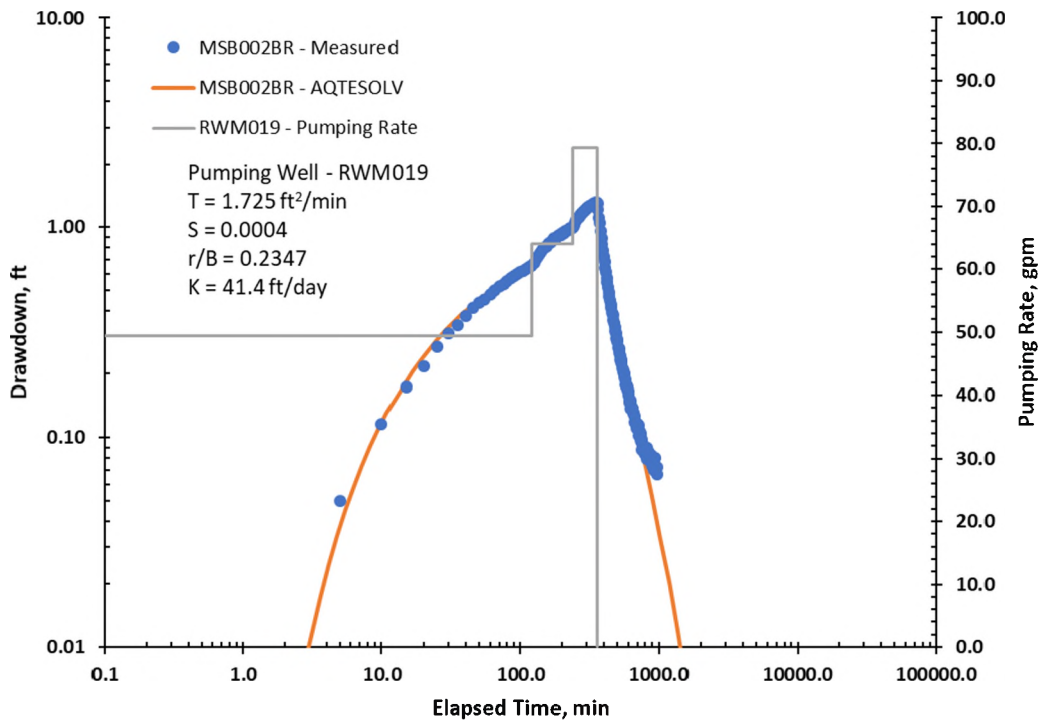


Figure 16. Step Test Drawdown Data and Hantush-Jacob Leaky Aquifer Type Curve for MSB002BR.

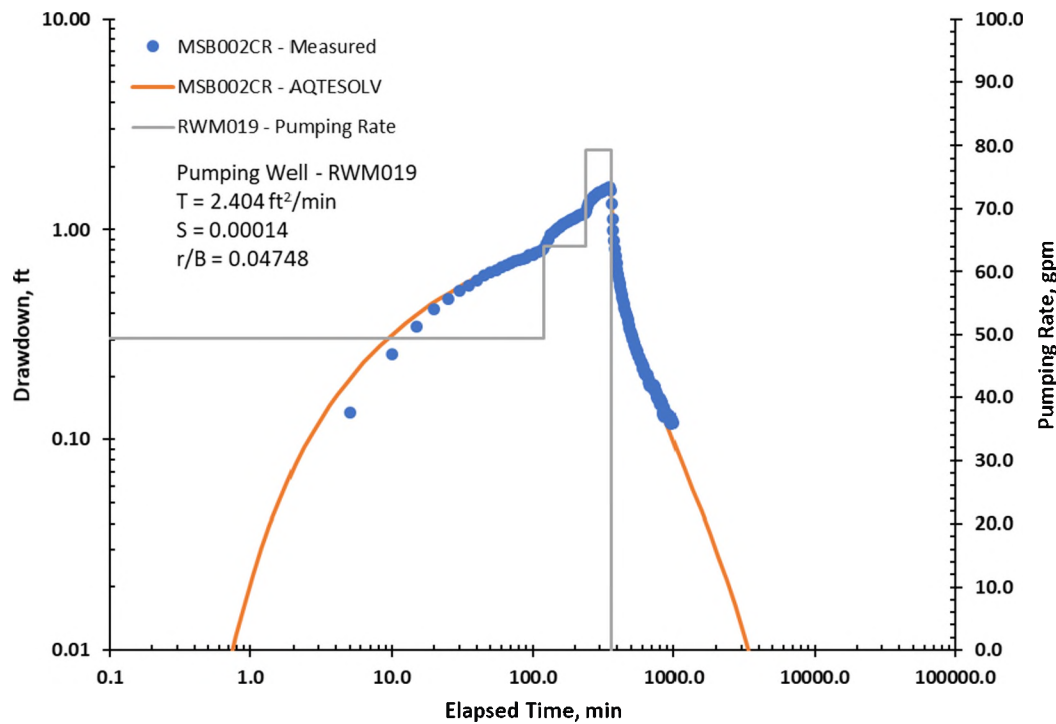


Figure 17. Step Test Drawdown Data and Hantush-Jacob Leaky Aquifer Type Curve for MSB002CR.

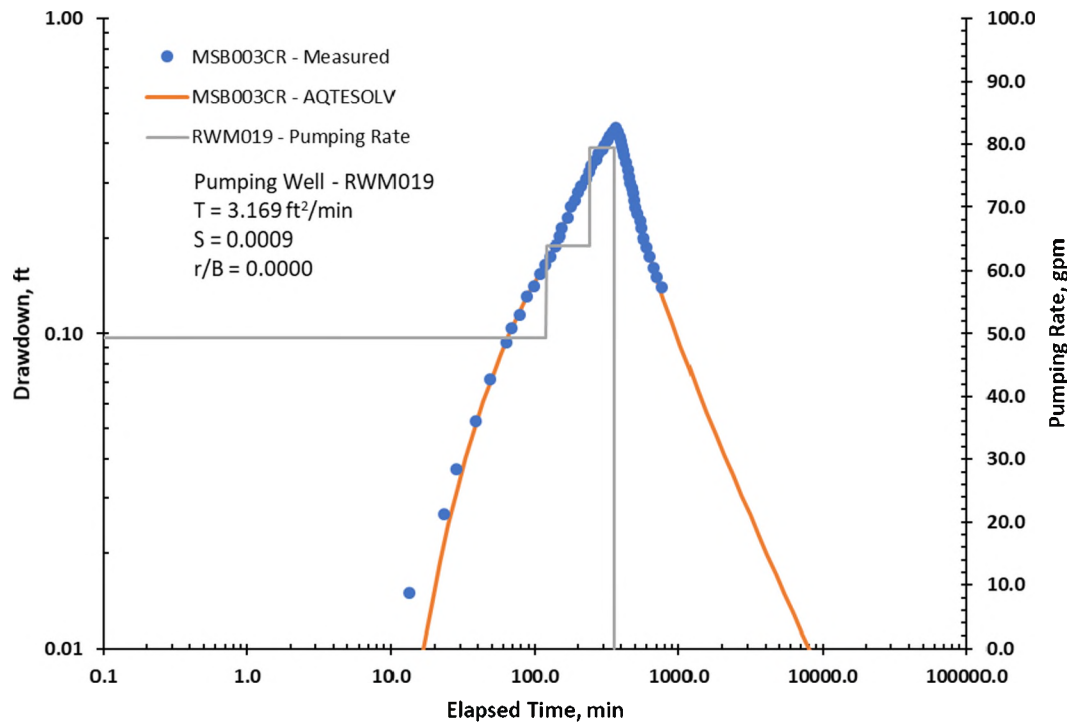


Figure 18. Step Test Drawdown Data and Hantush-Jacob Leaky Aquifer Type Curve for MSB003CR.

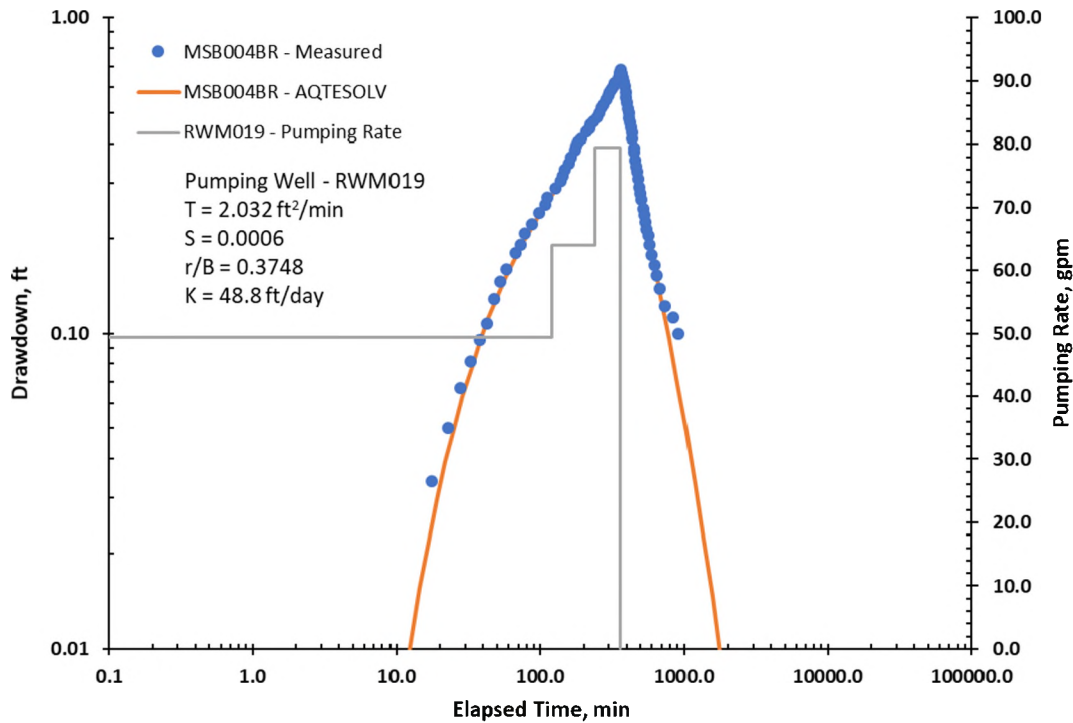


Figure 19. Step Test Drawdown Data and Hantush-Jacob Leaky Aquifer Type Curve for MSB004BR.

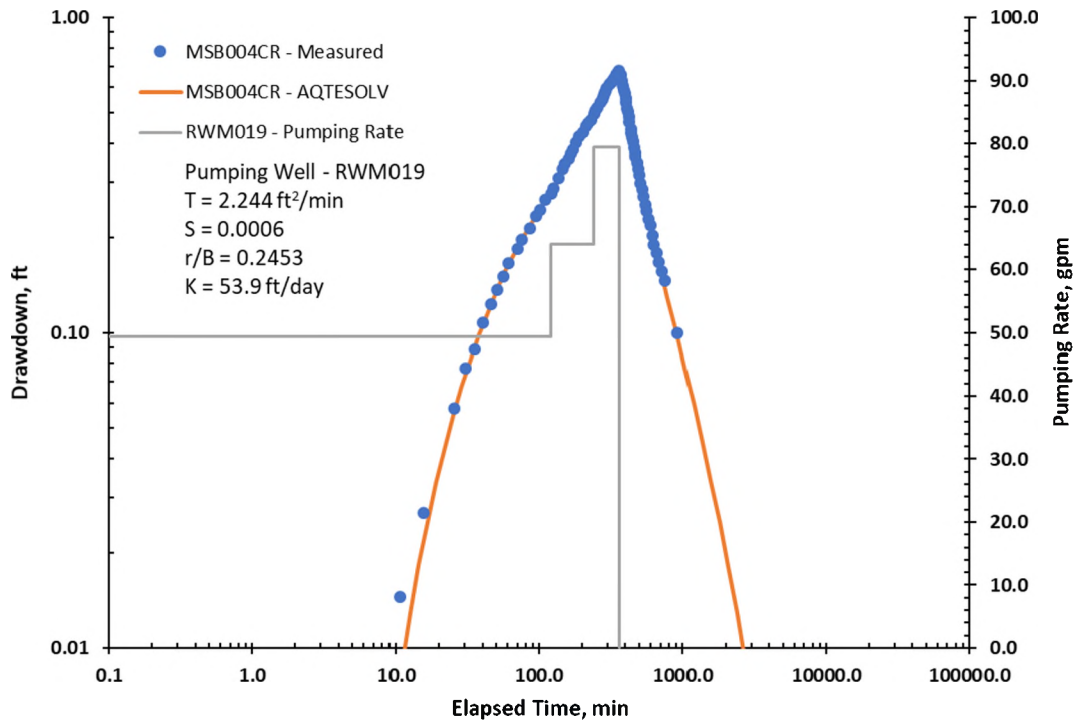


Figure 20. Step Test Drawdown Data and Hantush-Jacob Leaky Aquifer Type Curve for MSB004CR.

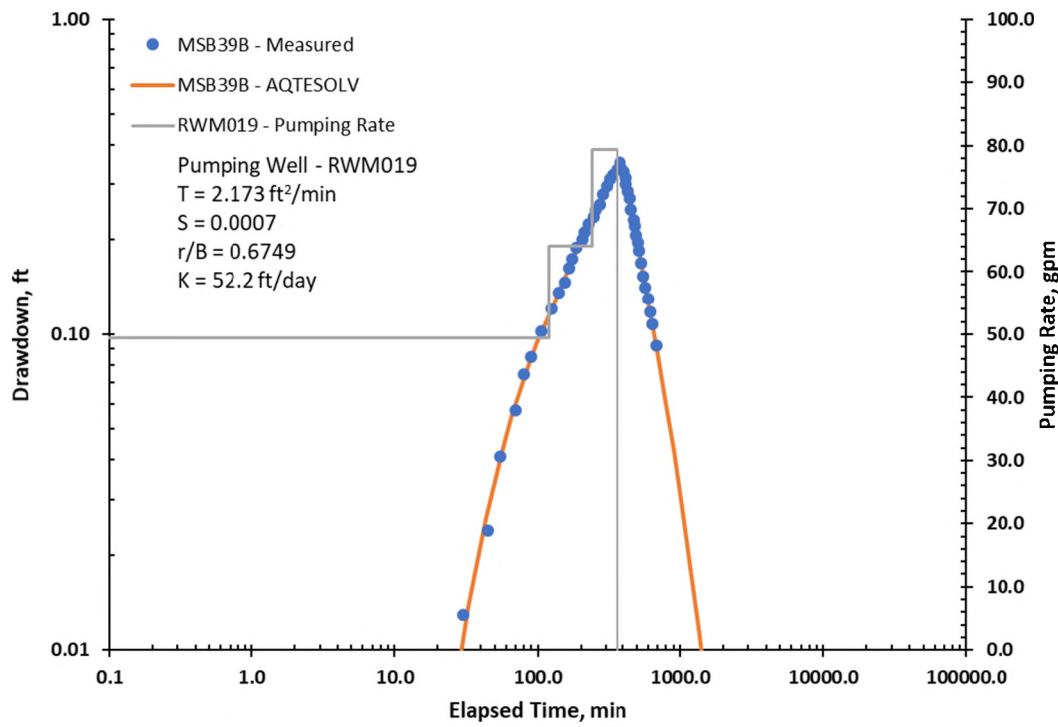


Figure 21. Step Test Drawdown Data and Hantush-Jacob Leaky Aquifer Type Curve for MSB39B.

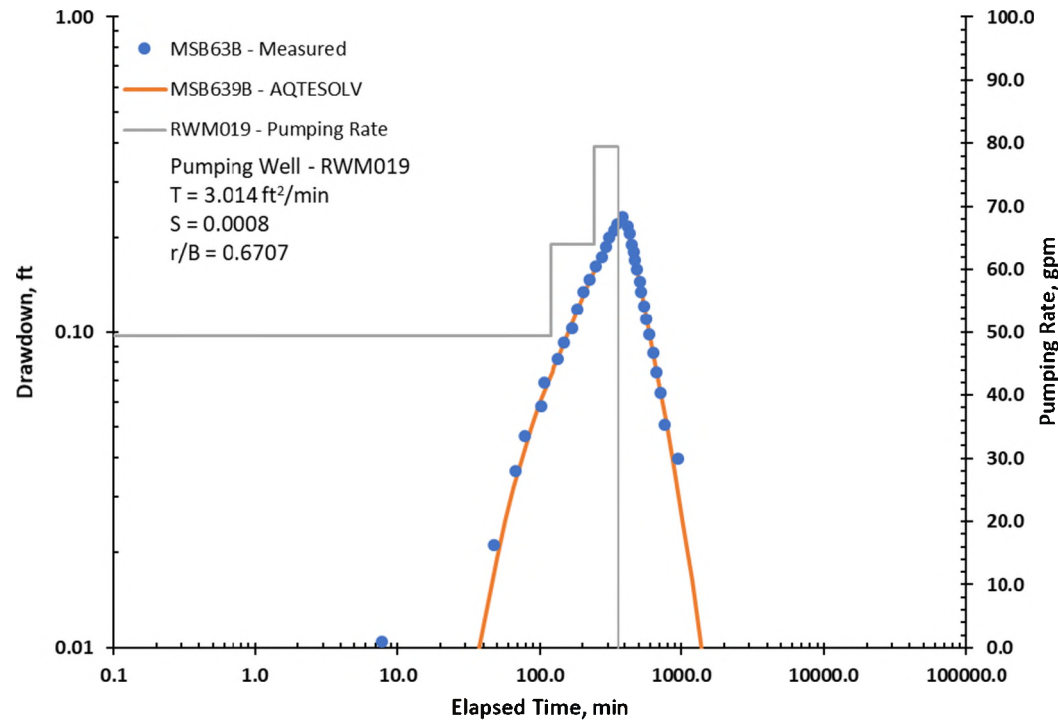


Figure 22. Step Test Drawdown Data and Hantush-Jacob Leaky Aquifer Type Curve for MSB63B.

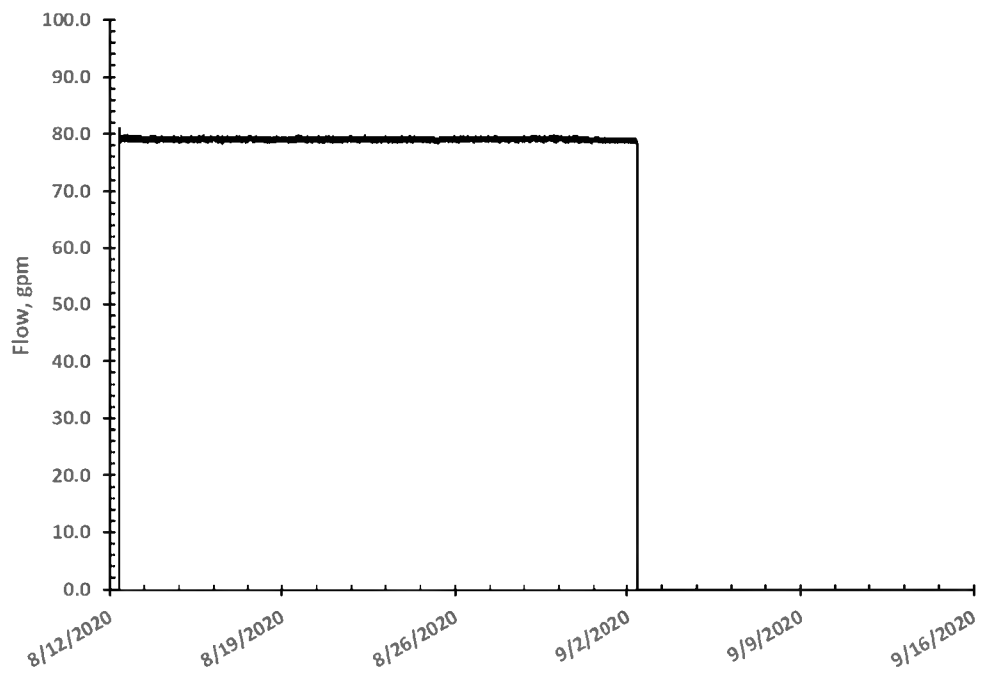


Figure 23. RWM019 Flow Rate During Constant Pumping Rate Aquifer Test.

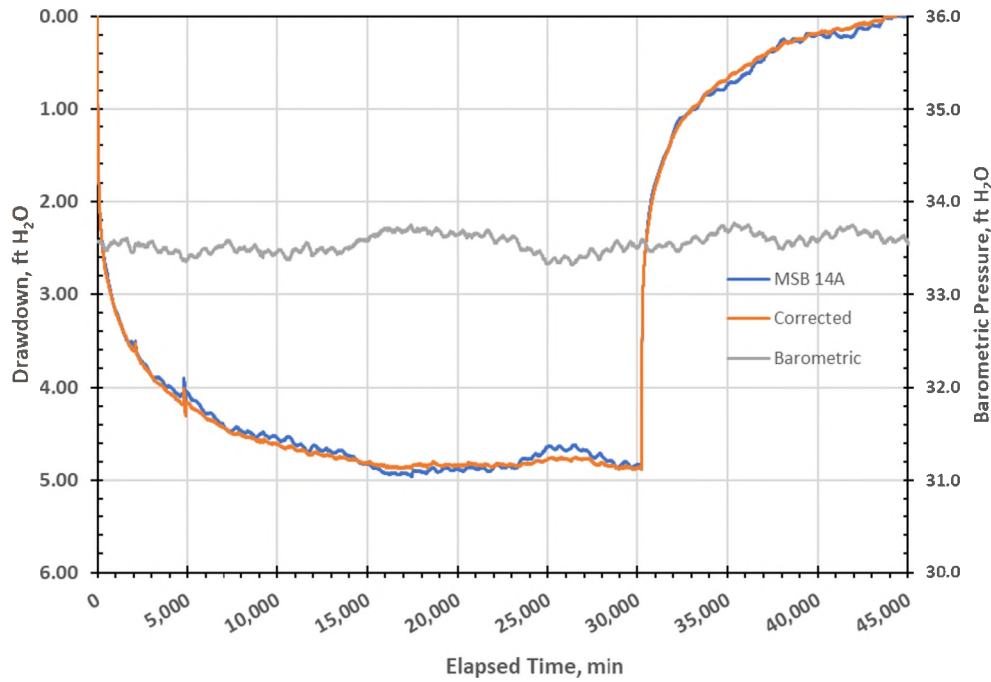


Figure 24. Drawdown as a Function of Elapsed Time for MSB 14A.

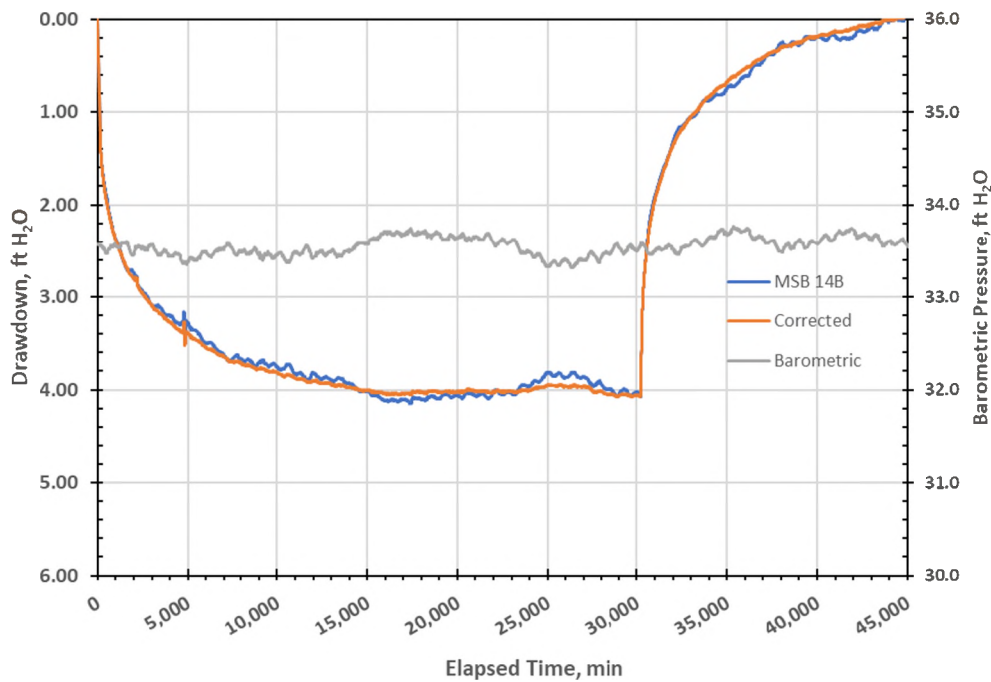


Figure 25. Drawdown as a Function of Elapsed Time for MSB 14B.

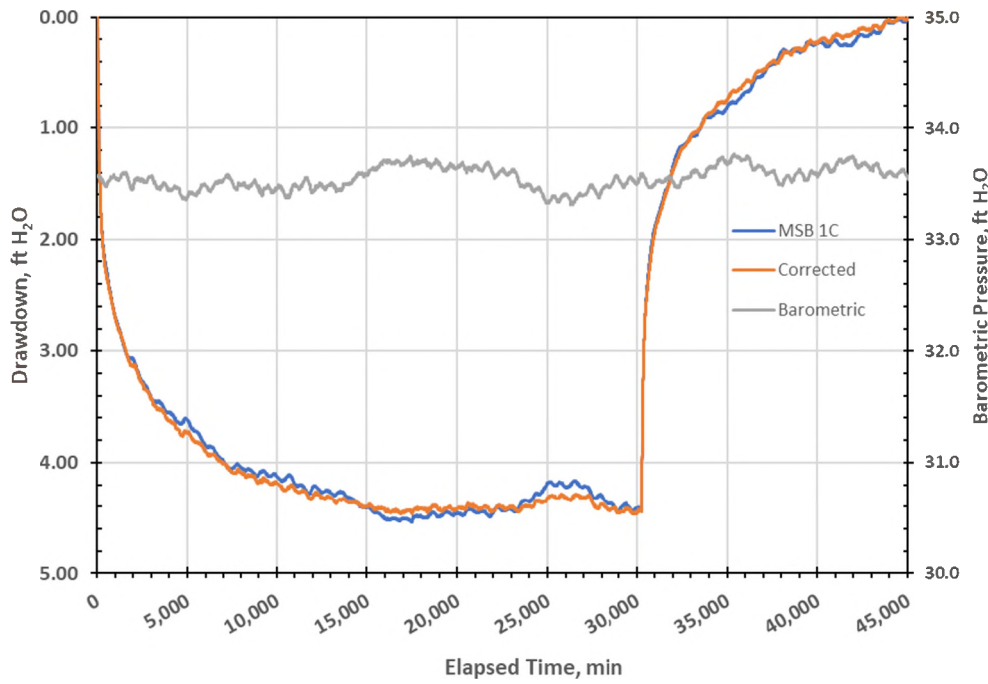


Figure 26. Drawdown as a Function of Elapsed Time for MSB 1C.

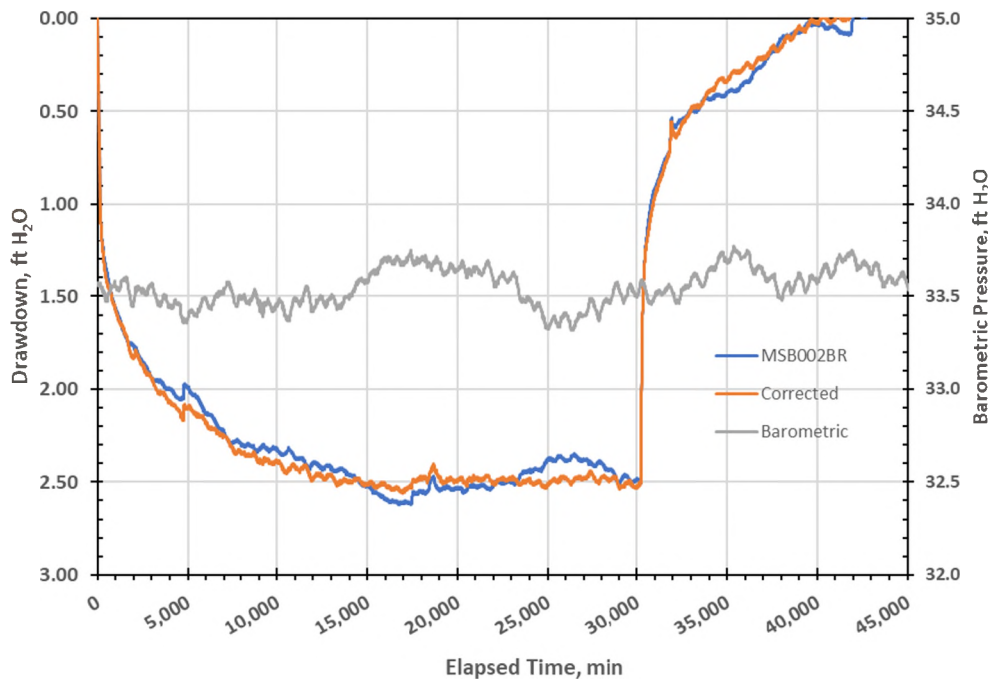


Figure 27. Drawdown as a Function of Elapsed Time for MSB002BR.

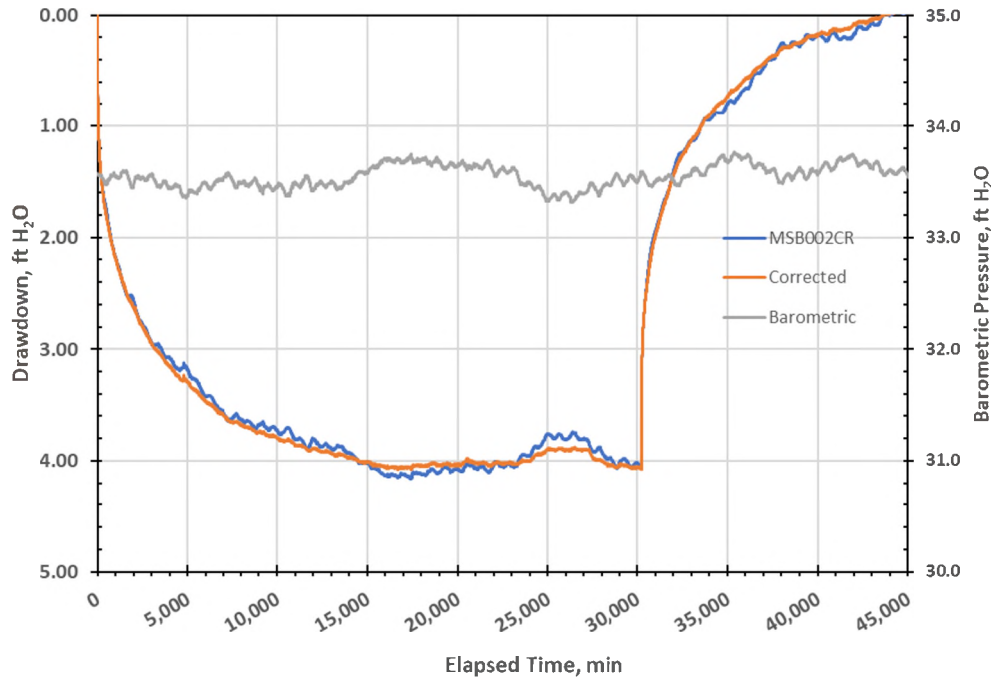


Figure 28. Drawdown as a Function of Elapsed Time for MSB002CR.

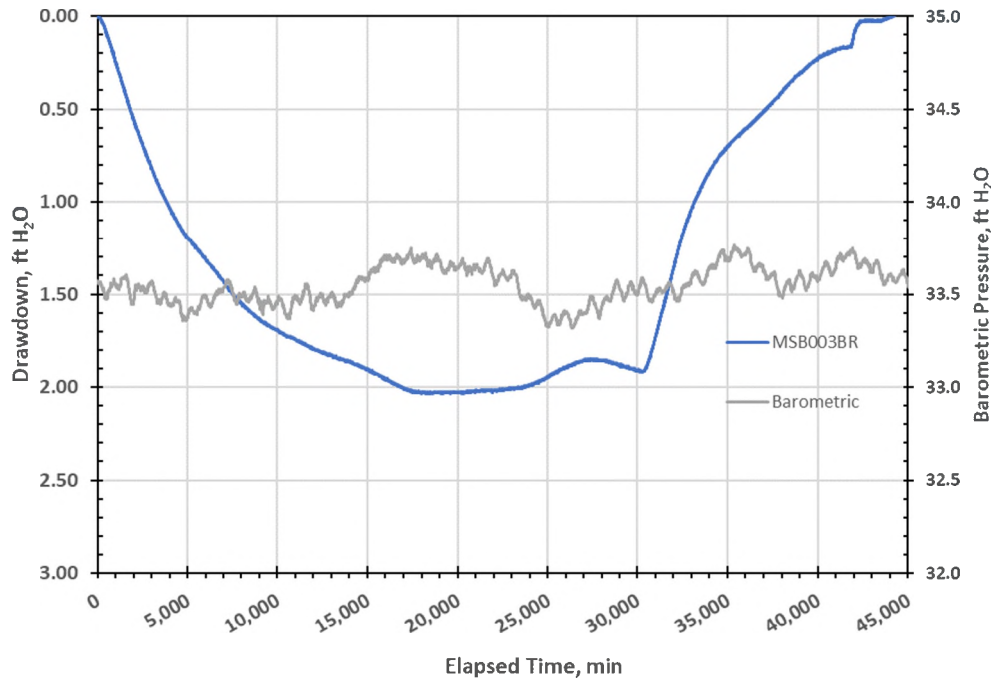


Figure 29. Drawdown as a Function of Elapsed Time for MSB003BR.

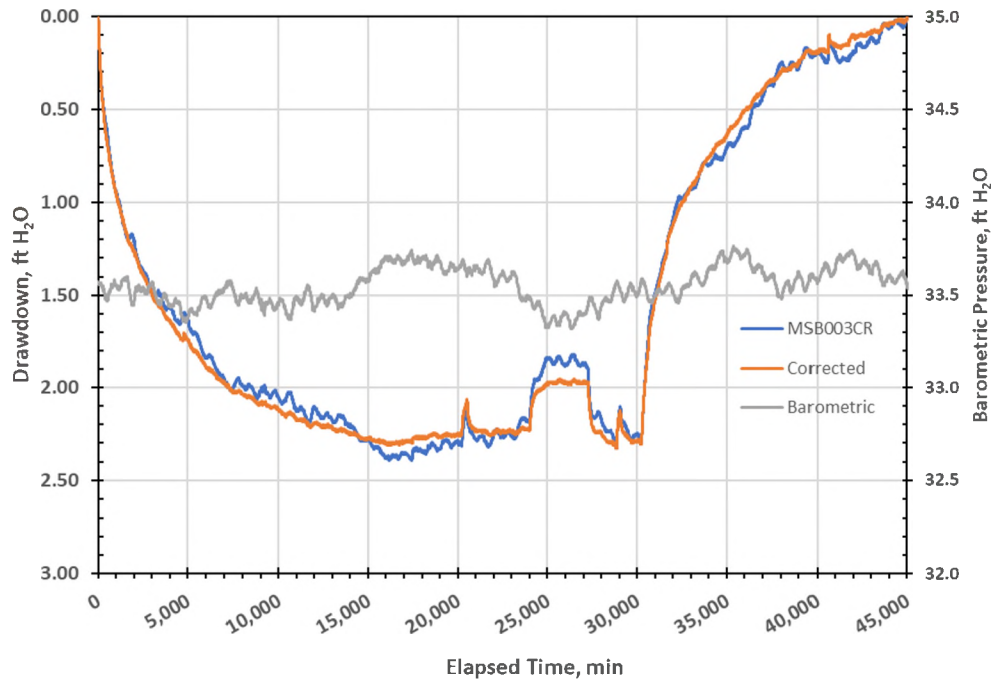


Figure 30. Drawdown as a Function of Elapsed Time for MSB003CR.

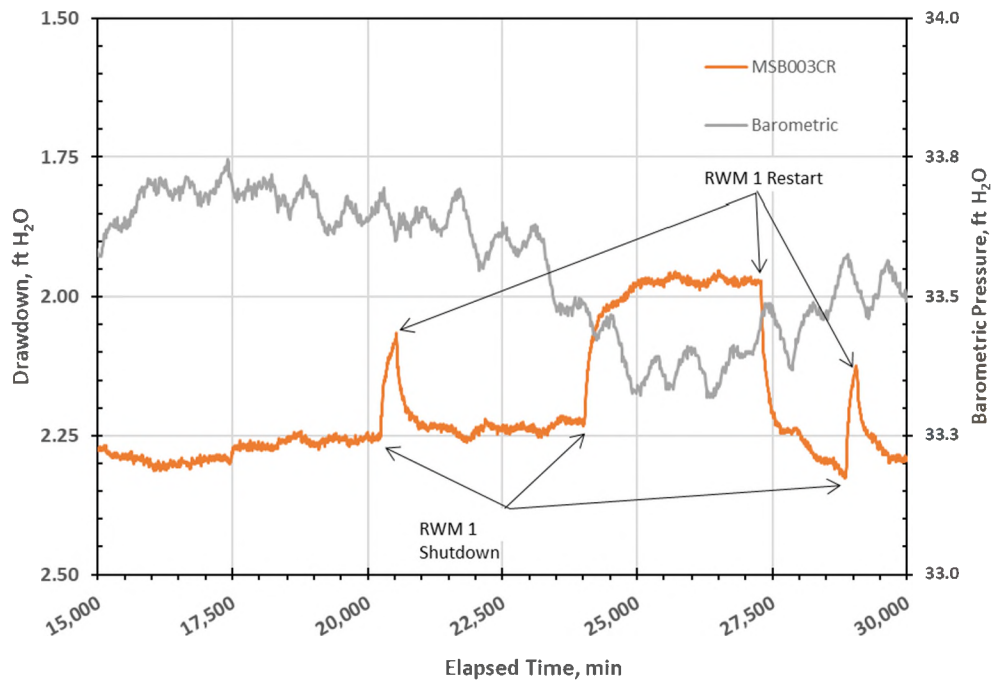


Figure 31. Effect of RWM 1 Shutdown/Restart on MSB003CR.

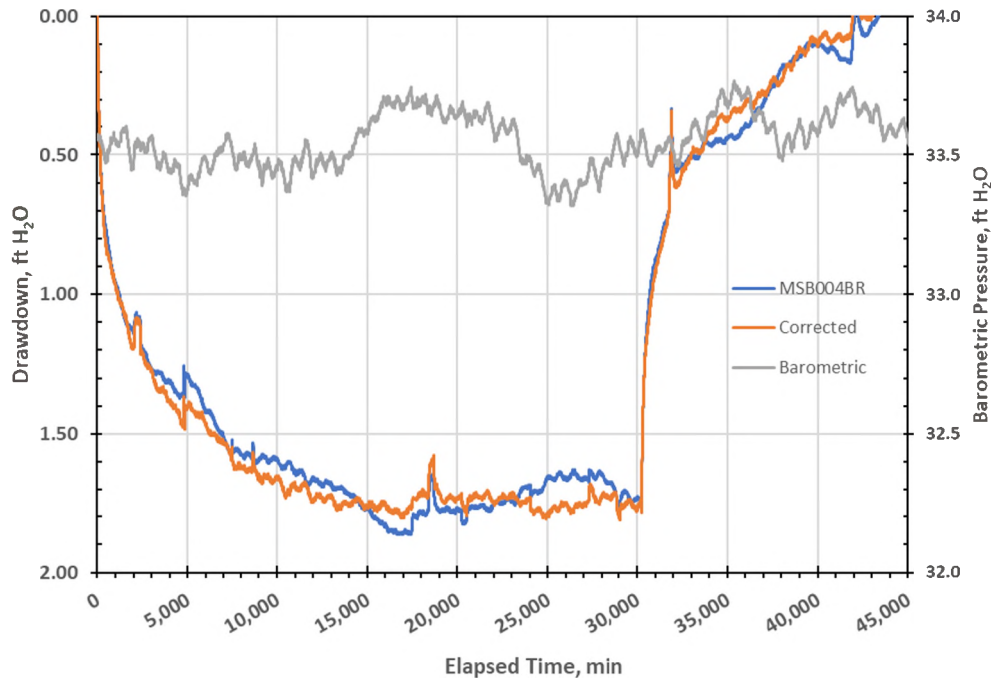


Figure 32. Drawdown as a Function of Elapsed Time for MSB004BR.

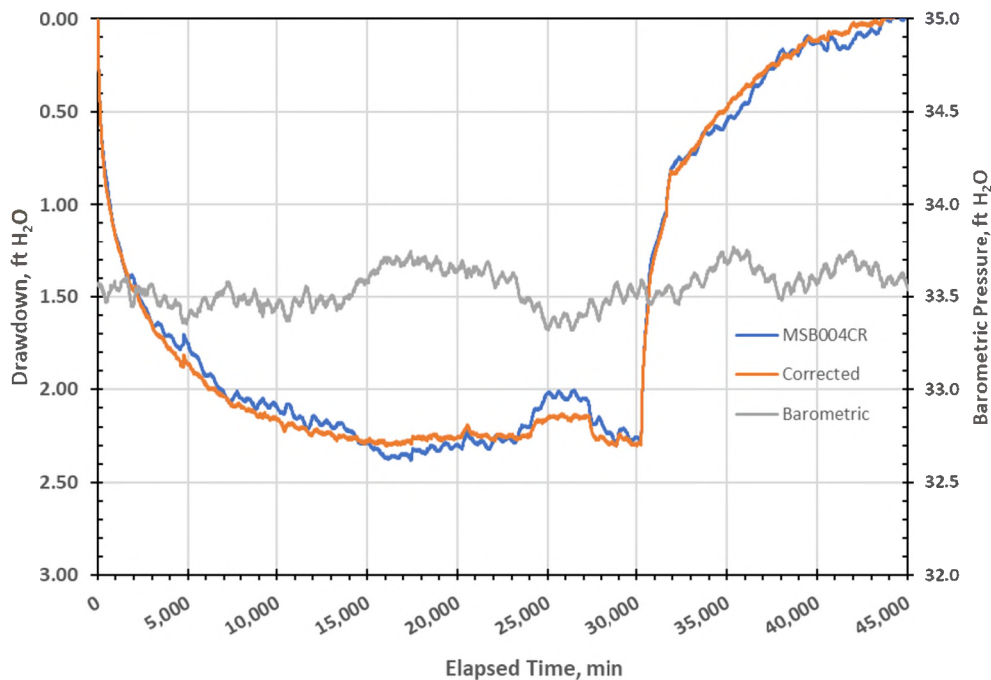


Figure 33. Drawdown as a Function of Elapsed Time for MSB004CR.

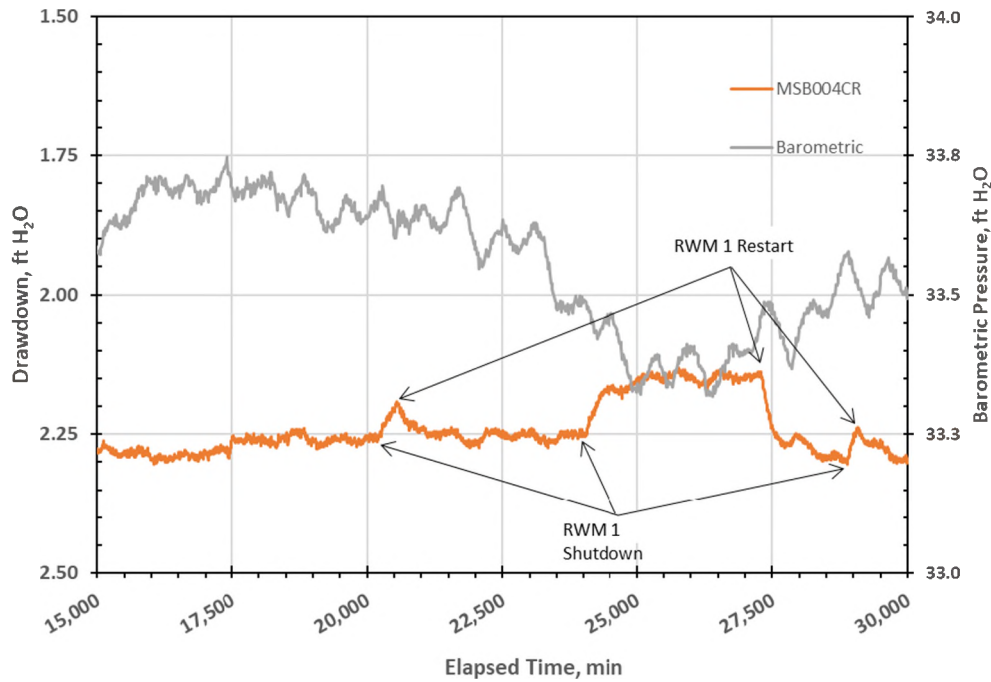


Figure 34. Effect of RWM 1 Shutdown/Restart on MSB004CR

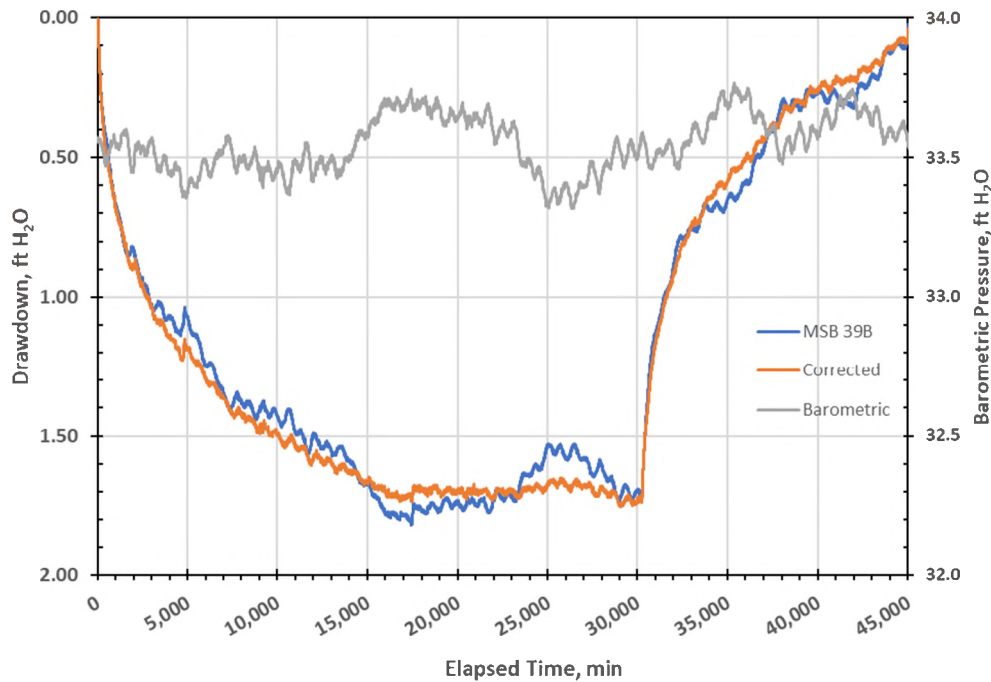


Figure 35. Drawdown as a Function of Elapsed Time for MSB 39B

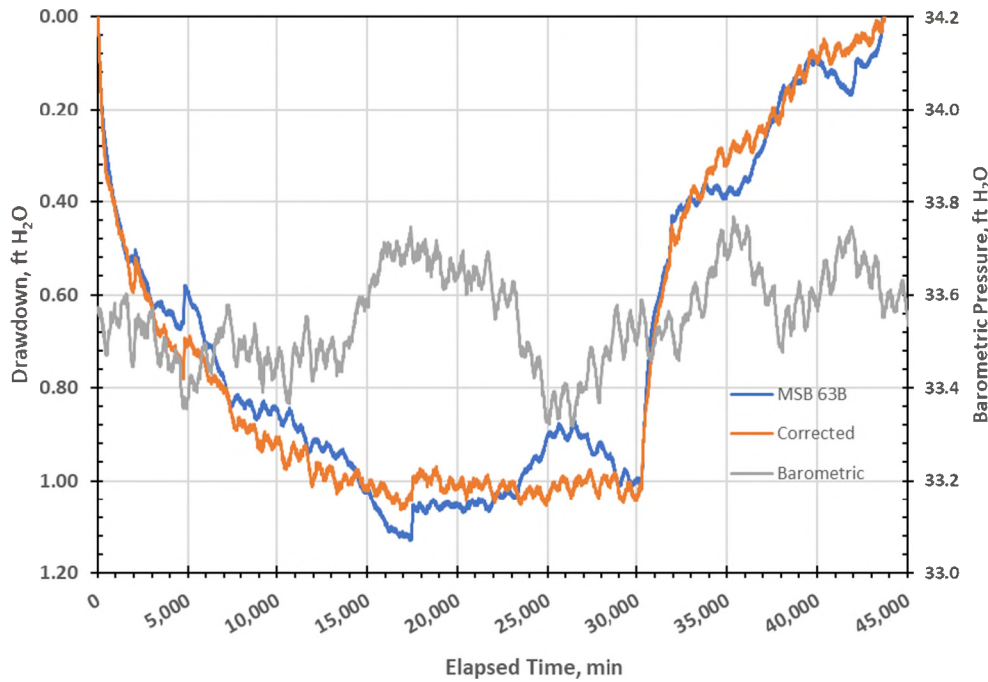


Figure 36. Drawdown as a Function of Elapsed Time for MSB 63B



Figure 37. Influence of Unidentified Well on Drawdown at MSB 63B.

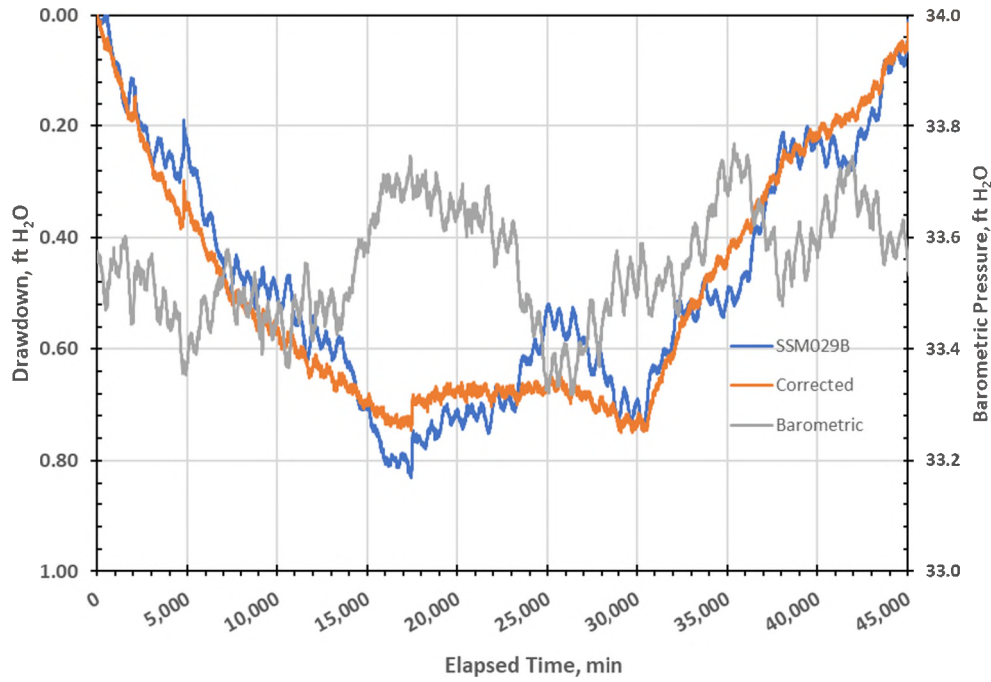


Figure 38. Drawdown as a Function of Elapsed Time for SSM029B.

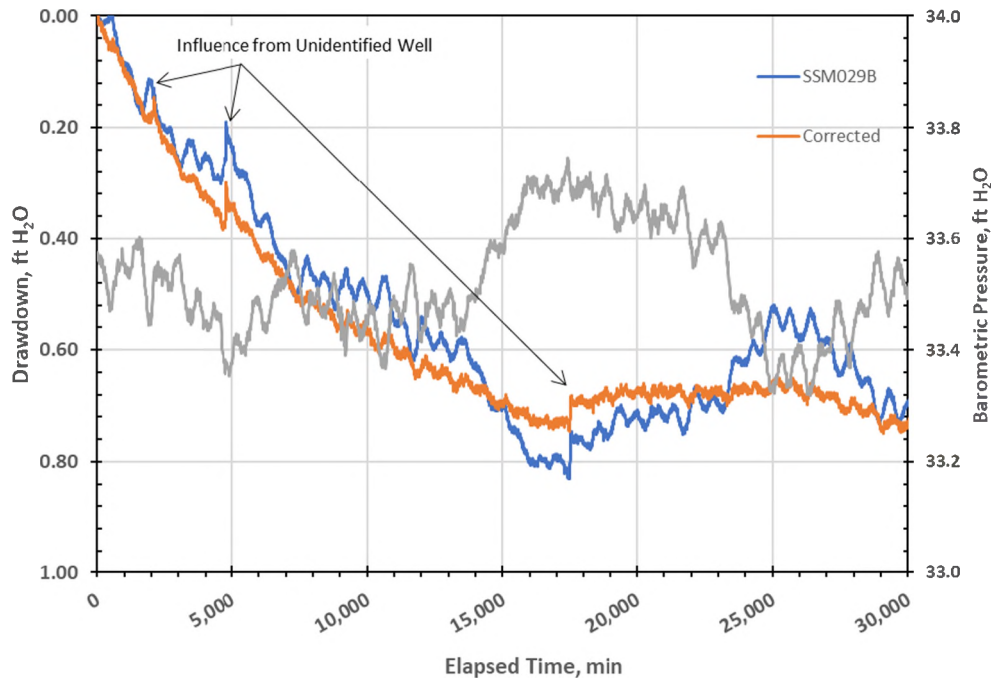


Figure 39. Influence of Unidentified Well on Drawdown at SSM029B.

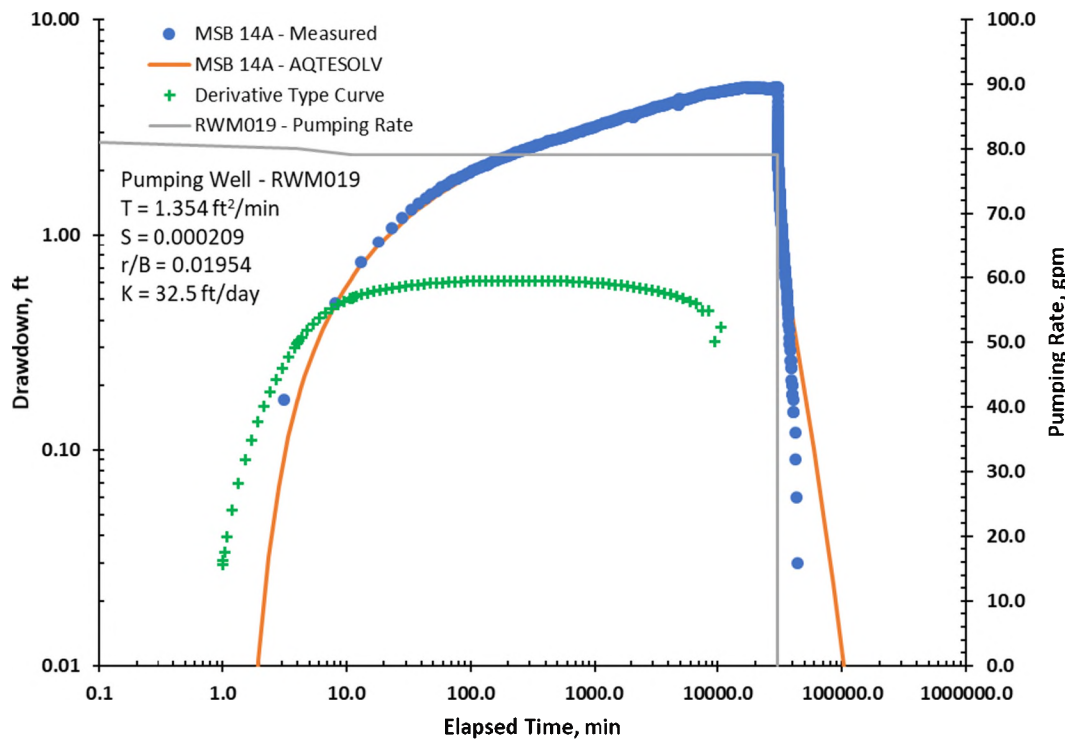


Figure 40. Drawdown Data and Hantush-Jacob Leaky Aquifer Type Curve for MSB14A.

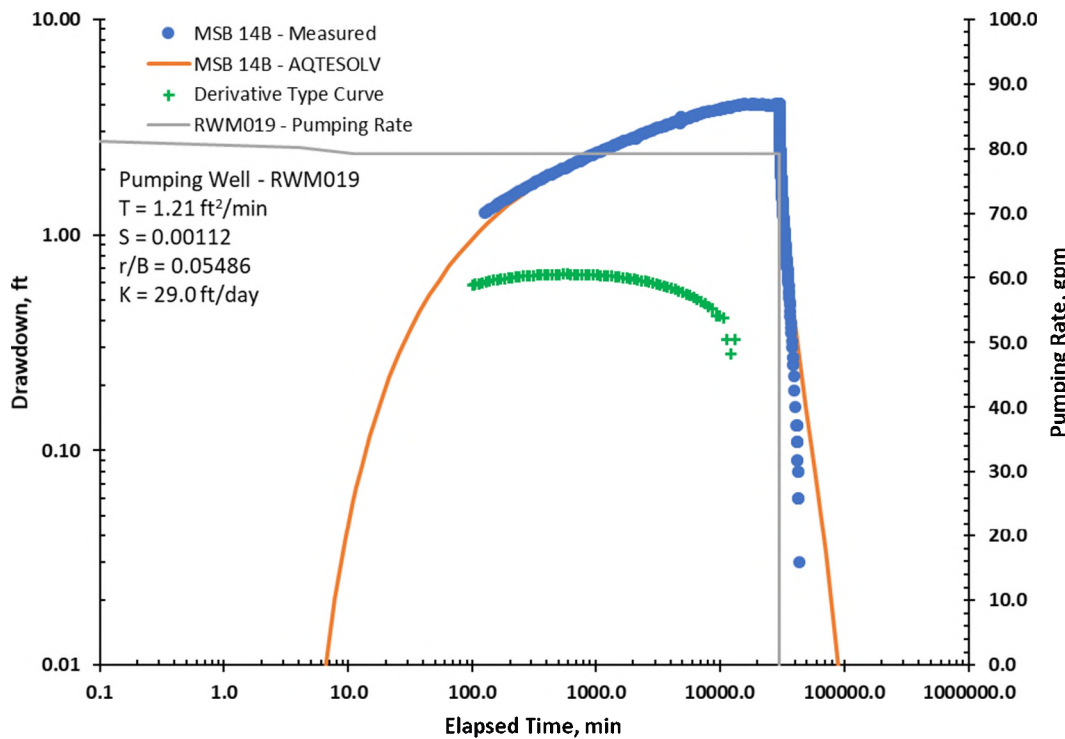


Figure 41. Drawdown Data and Hantush-Jacob Leaky Aquifer Type Curve for MSB14B.

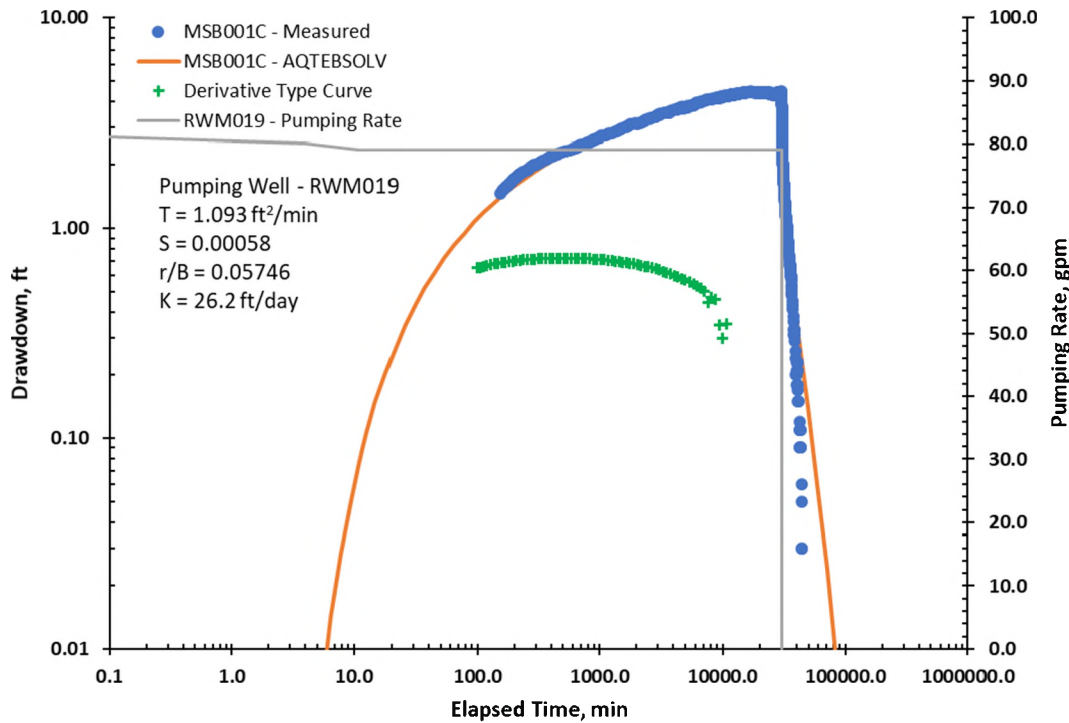


Figure 42. Drawdown Data and Hantush-Jacob Leaky Aquifer Type Curve for MSB001C.

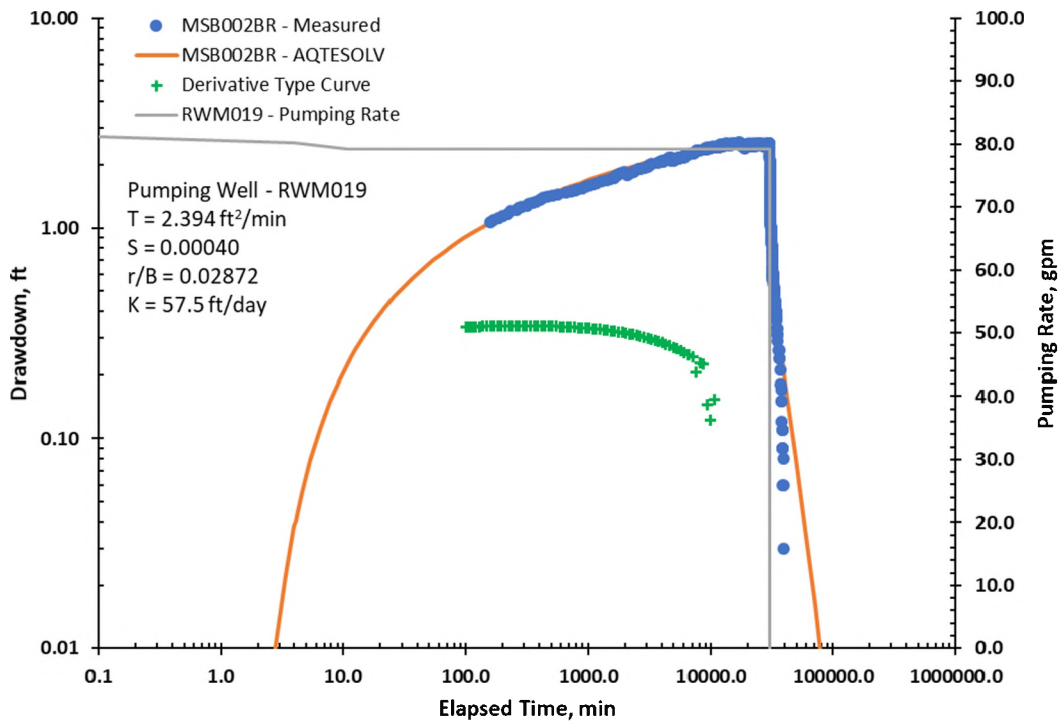


Figure 43. Drawdown Data and Hantush-Jacob Leaky Aquifer Type Curve for MSB002BR.

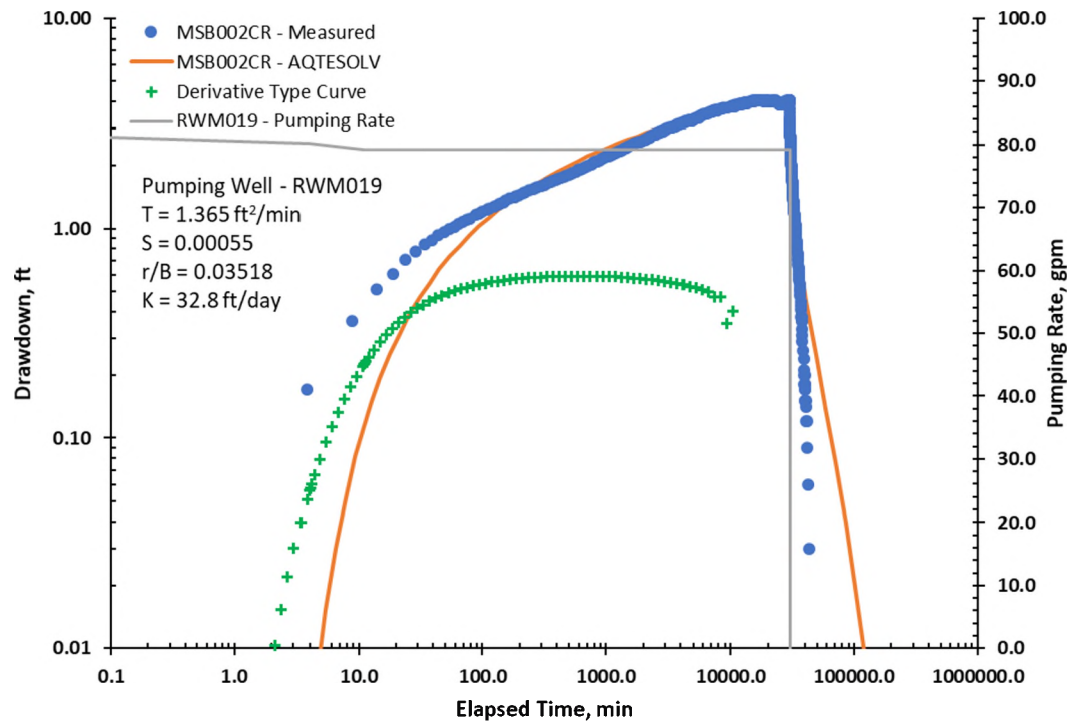


Figure 44. Drawdown Data and Hantush-Jacob Leaky Aquifer Type Curve for MSB002CR.

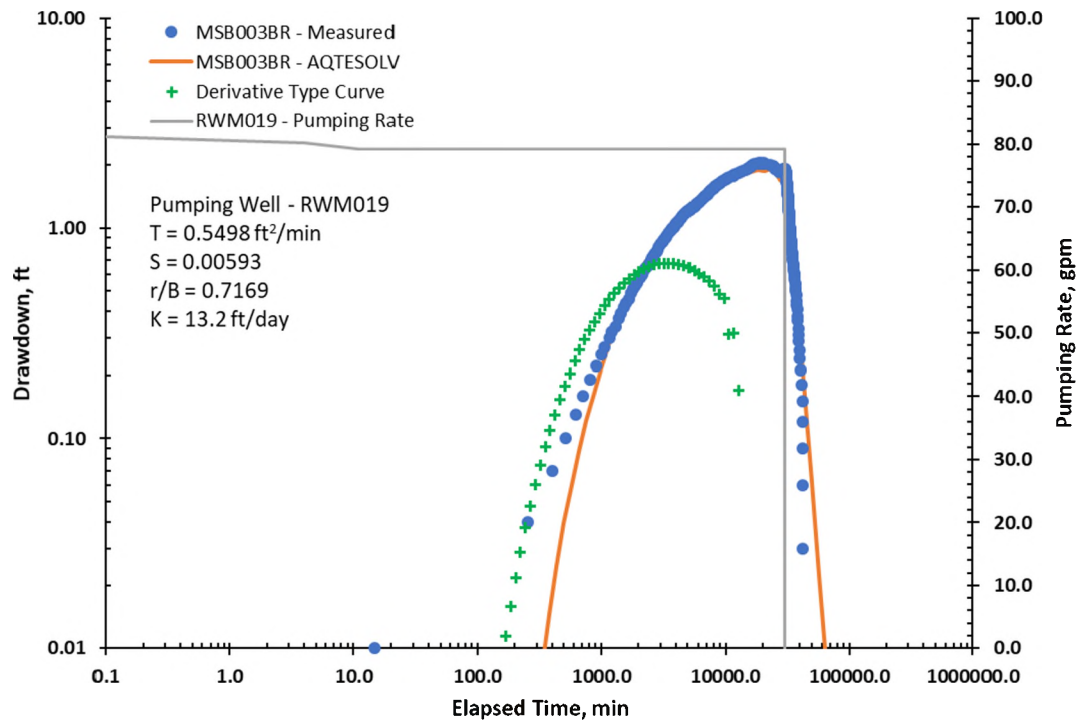


Figure 45. Drawdown Data and Hantush-Jacob Leaky Aquifer Type Curve for MSB003BR.

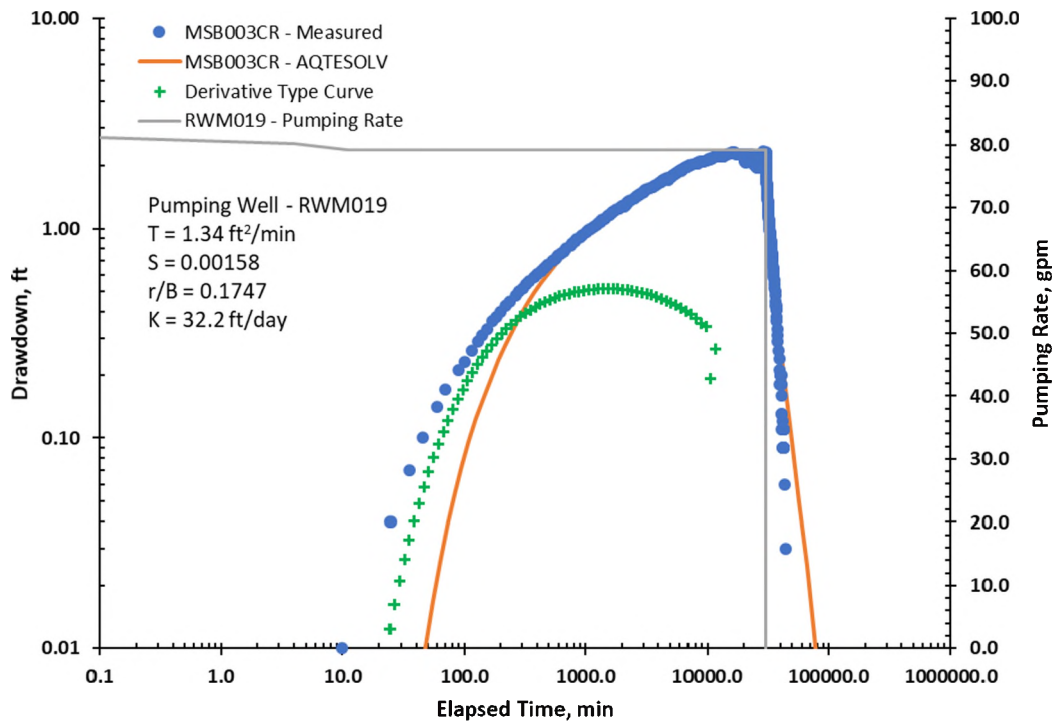


Figure 46. Drawdown Data and Hantush-Jacob Leaky Aquifer Type Curve for MSB003CR.

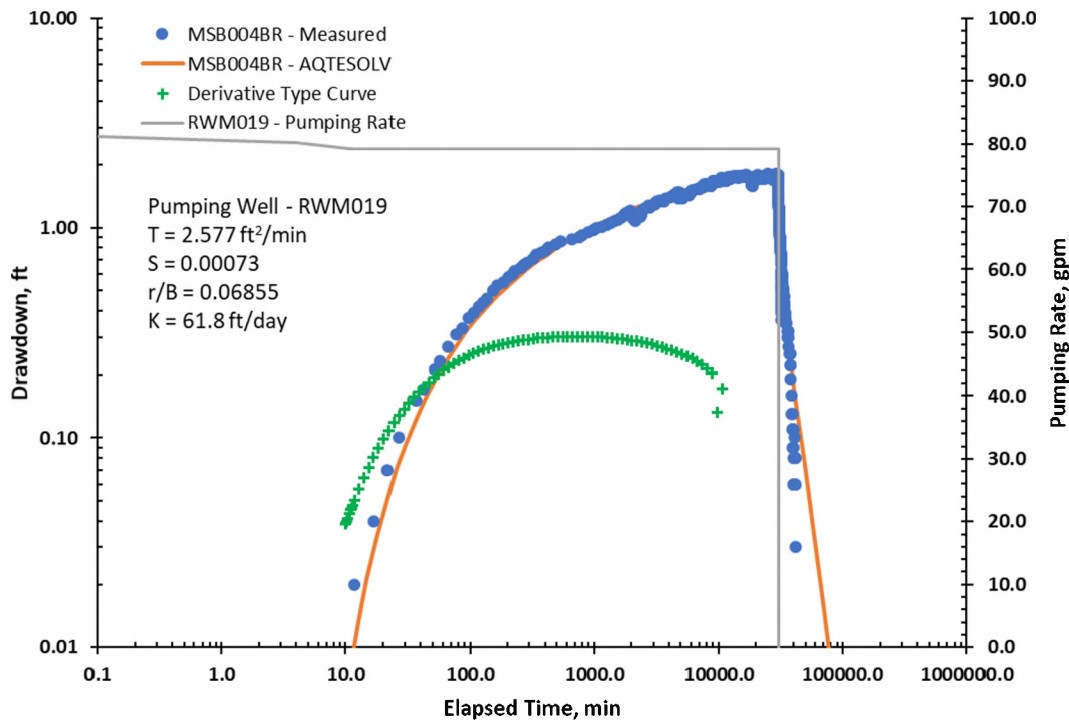


Figure 47. Drawdown Data and Hantush-Jacob Leaky Aquifer Type Curve for MSB004BR.

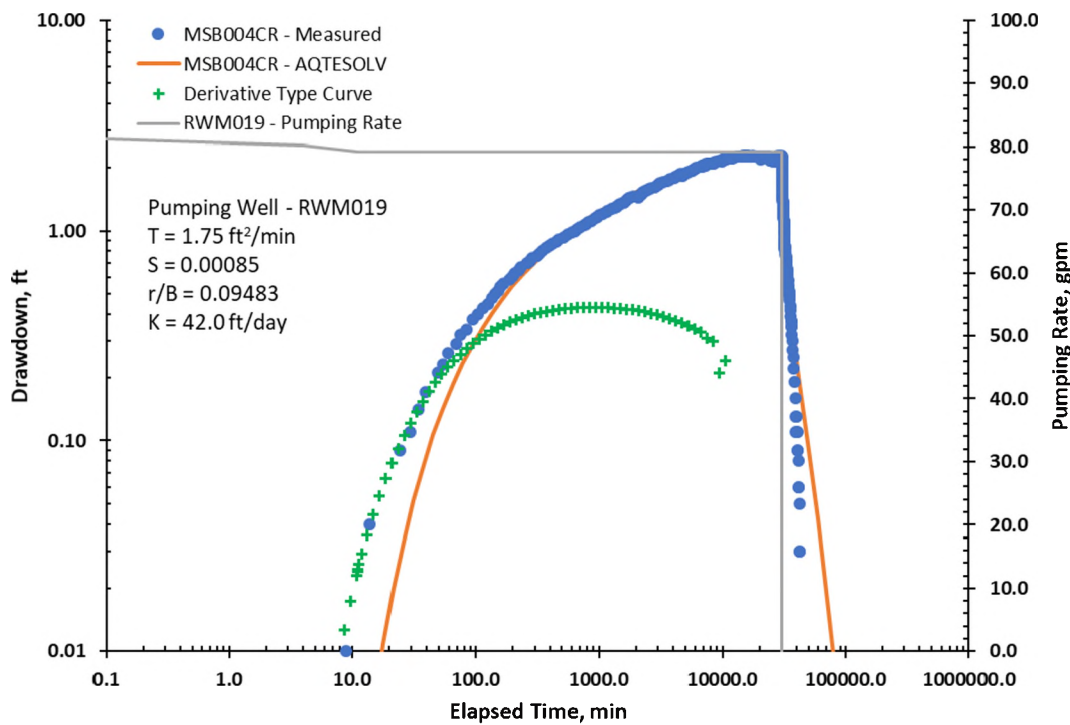


Figure 48. Drawdown Data and Hantush-Jacob Leaky Aquifer Type Curve for MSB004CR.

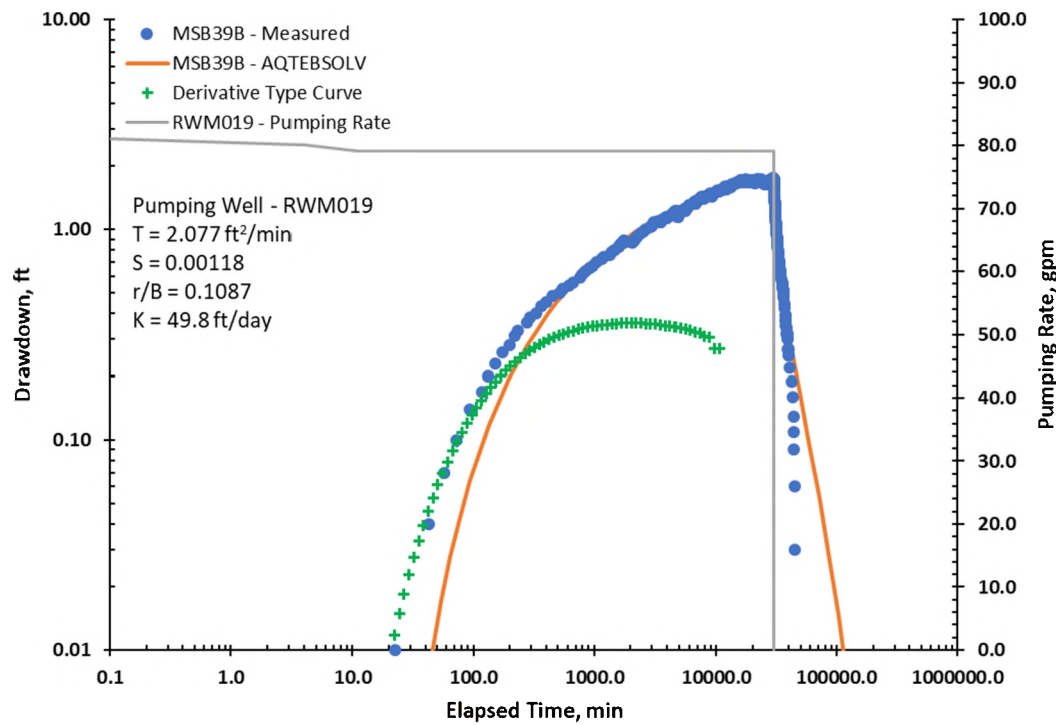


Figure 49. Drawdown Data and Hantush-Jacob Leaky Aquifer Type Curve for MSB 39B.

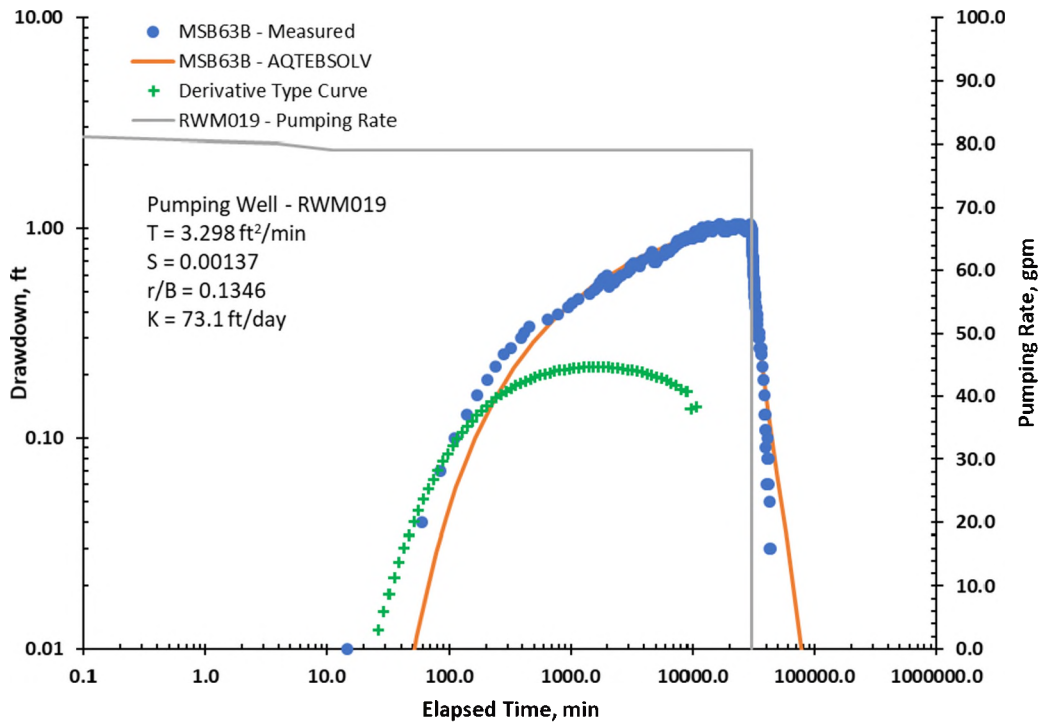


Figure 50. Drawdown Data and Hantush-Jacob Leaky Aquifer Type Curve for MSB 63B.

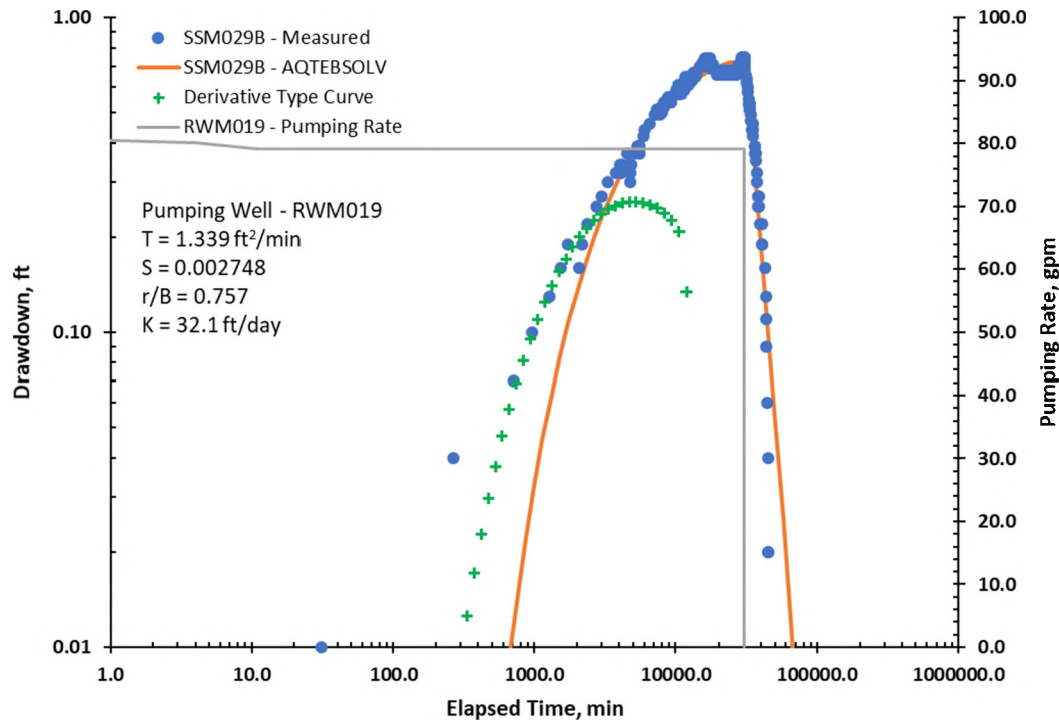


Figure 51. Drawdown Data and Hantush-Jacob Leaky Aquifer Type Curve for SSM029B.

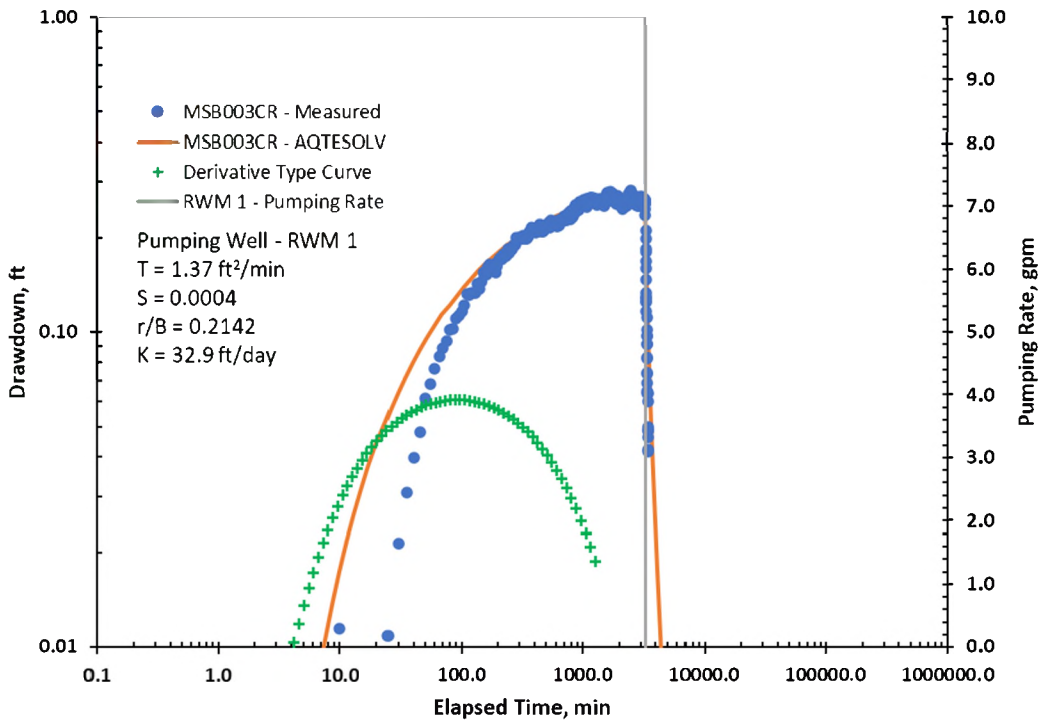


Figure 52. Drawdown Data and Hantush-Jacob Leaky Aquifer Type Curve for MSB003CR with RWM 1 as Pumping Well.

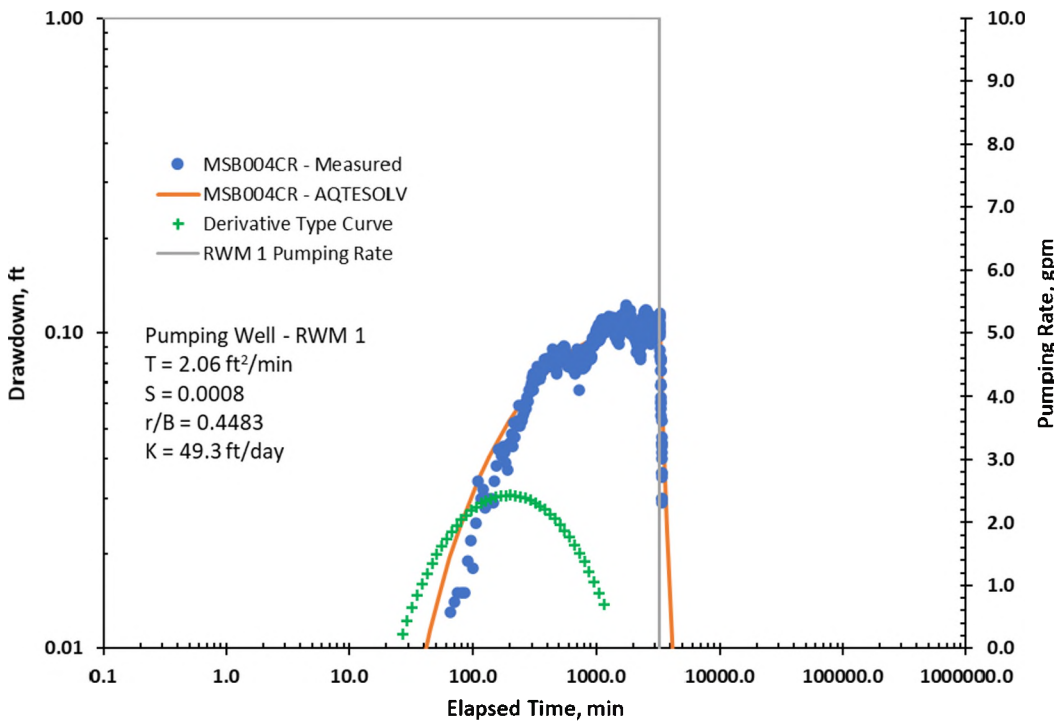


Figure 53. Drawdown Data and Hantush-Jacob Leaky Aquifer Type Curve for MSB004CR with RWM 1 as Pumping Well.

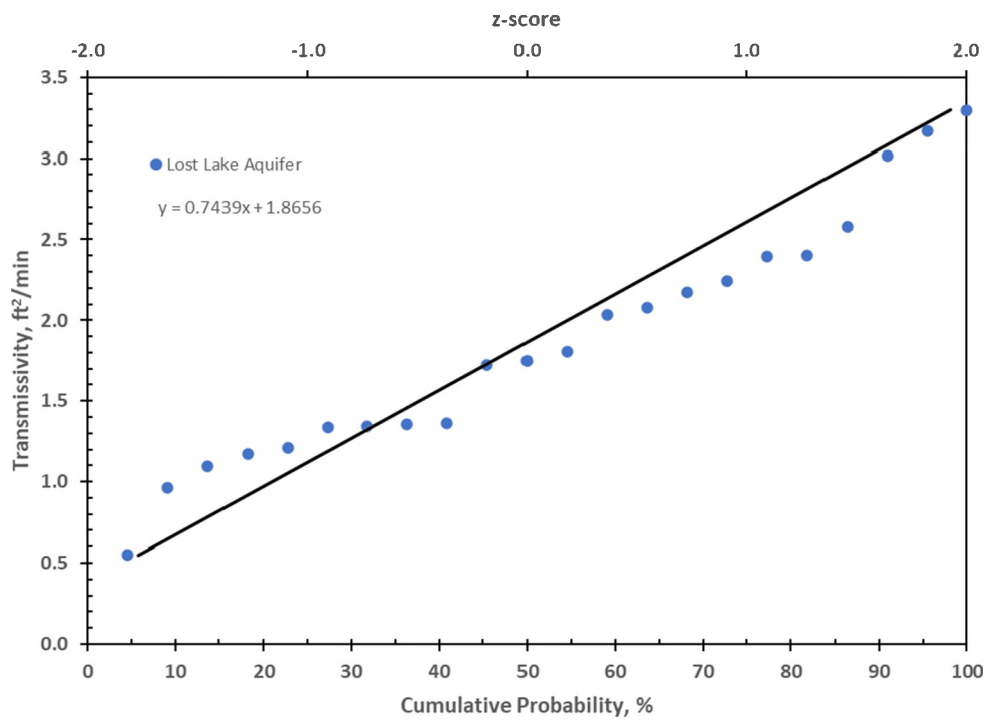


Figure 54. Cumulative Probability Plot of Transmissivity for the Lost Lake Aquifer Near RWM019

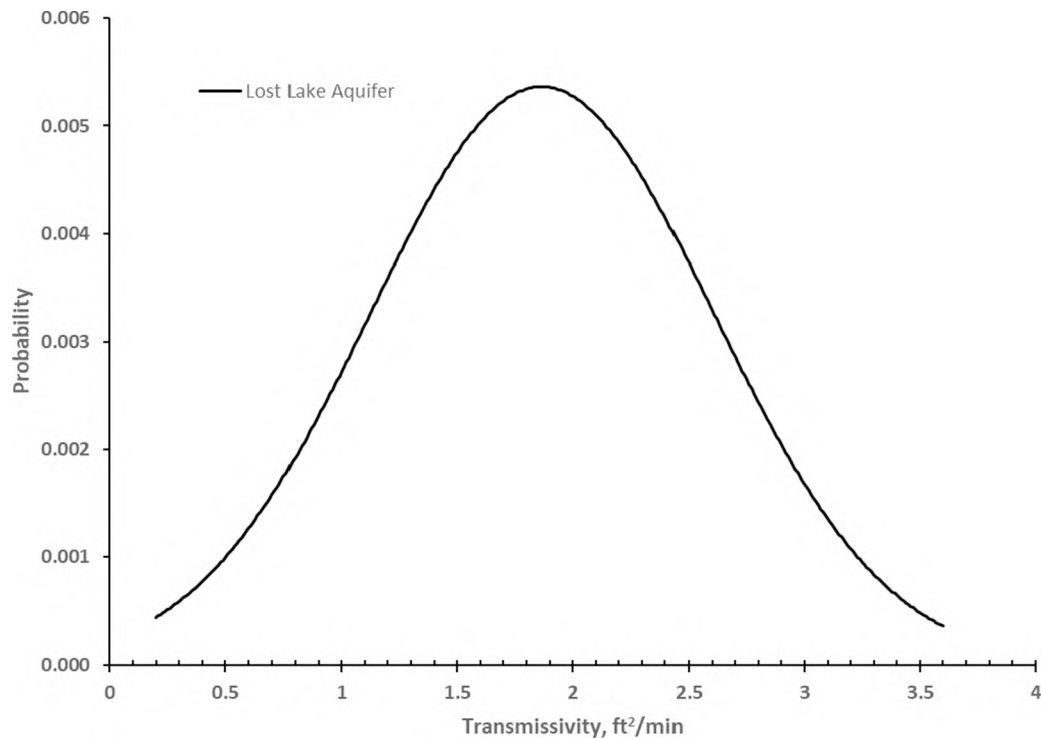


Figure 55. Probability Density Function for Transmissivity of the Lost Lake Aquifer Near RWM019.

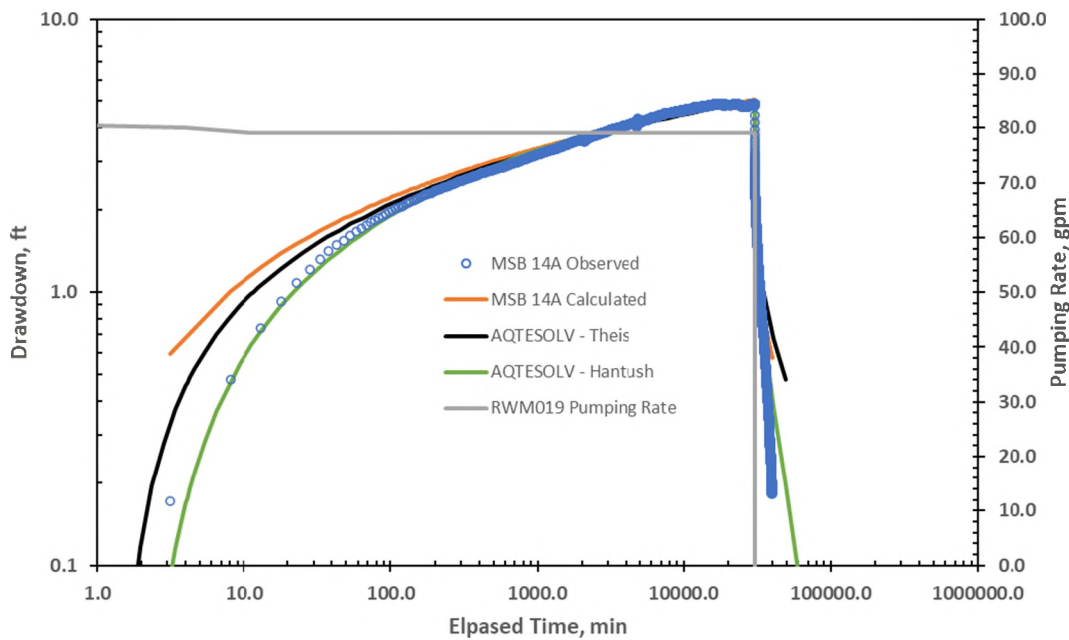


Figure 56. Drawdown as a Function of Time for MSB 14A Using Theis Solution (spreadsheet calculation for verification).

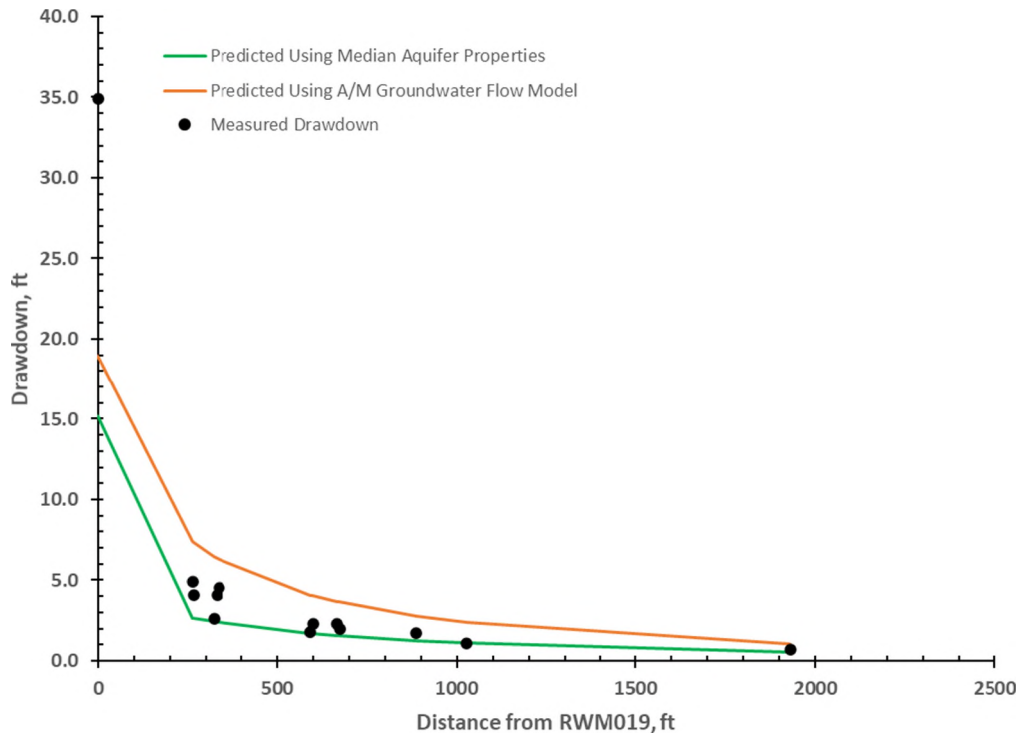


Figure 57. Comparison of Measured and Predicted Drawdown.

Table 1. Previously Reported Hydraulic Properties of the Lost Lake Aquifer Zone

Well ^a	T ^b (ft ² /min)	S ^b	r/B ^c	Observed Specific Capacity (gpm/ft)	Well Efficiency (%)
RWM 1 ^a	2.32	0.001	-	0.9	-
RWM 2 ^a	2.32	0.001	-	0.6	-
RWM 3 ^a	2.32	0.001	-	4.2	-
RWM 3 ^{c,f,g}	0.992	0.019	0.0006	4.0	67
RWM 4 ^a	1.11	0.001	-	4.3	82
				3.9	75
				4.6	62
RWM 5 ^a	3.53	0.00005	-	5.3	79
				5.8	65
				5.9	55
RWM 5 ^{c,f,g}	0.992	0.019	0.0006	3.3	61
RWM 6 ^a	1.76	0.0006	-	2.8	-
RWM 7 ^a	1.95	0.0006	-	1.9	78
				1.8	64
				1.4	52
RWM 8 ^a	1.49	0.001	-	5.3	75
				5.7	64
				4.3	53
RWM 8 ^{d,f}	0.946	0.002	0.2181	4.5	88
RWM 9 ^a	10.49	0.01	-	6.5	91
				6.8	87
				7.8	81
RWM 10 ^a	2.32	0.0009	-	3.1	88
				2.9	85
				3.4	81
				2.8	75
				2.6	69
RWM 11 ^a	9.10	0.0003	-	4.0	90
				4.3	85
				4.0	81
RWM 16PA ^{b,f}	0.899	0.00065	0.0823	-	-
RWM 16PB ^{b,f}	0.826	0.00073	0.0460	-	-
RWM018 ^{c,f}	0.816	0.00047	0.2461	3.22	69.6
MSB-40B ^{b,f}	0.782	0.00053	0.0458	-	-

Data compiled from ^aGeraghty and Miller (1987), ^bHiergesell (1992), ^cDixon (2018), and ^dDixon (2019).

^eValues determined using Theis confined aquifer method unless otherwise noted.

^fValues determined using Hantush-Jacob leaky confined aquifer method (1955, 1961a and b).

^gRWM 3 and RWM 5 tested together.

Table 2 Construction Details for Wells Used in Aquifer Test at RWM019

Well Name	Distance from RWM019 (ft)	Diameter (in)	SRS East (ft)	SRS North (ft)	Top of Screen (ft msl)	Bottom of Screen (ft msl)	Top of Screen (ft bgs)	Bottom of Screen (ft bgs)	Total Depth (ft)	Screen Length (ft)
RWM019	0	6	48785.0	101633.0	197.3	146.3	149.8	200.8	216.0	50
MSB 14A	263	4	48521.9	101629.4	164.6	144.6	182.0	202.0	204.1	20
MSB 14B	266	4	48519.1	101639.0	193.9	188.9	153.0	158.0	160.0	5
MSB002BR	323	2	48751.4	101954.6	157.8	147.8	195.0	205.0	219.0	10
MSB002CR	333	2	48757.9	101964.7	187.6	177.6	165.0	175.0	177.5	10
MSB 1C	338	4	48512.7	101832.4	166.0	161.3	187.0	191.7	193.8	5
MSB004BR	593	2	48290.2	101959.7	158.4	148.4	195.0	205.0	207.0	10
MSB004CR	600	2	48288.6	101970.6	188.0	178.0	165.5	175.5	177.5	10
MSB003BR	674	2	48496.7	102242.4	159.2	149.2	200.0	210.0	212.2	10
MSB003CR	668	2	48508.3	102241.4	187.3	177.3	172.0	182.0	184.2	10
MSB 39B	888	4	48376.9	100844.6	149.6	144.0	151.0	201.0	197.8	6
MSB 63B	1027	4	47861.0	101184.3	140.9	136.2	204.0	208.7	210.7	5
SSM029B	1930	2	49700.2	99934.3	164.9	154.9	160.8	170.8	173.0	10

¹Predicted using the A/M groundwater flow model (SRNS, 2017)

Table 3. Calculated Barometric Efficiencies for RWM019 and Nearby Observation Wells.

Well ID	Barometric Efficiency (%)
MSB 14A	65
MSB 14B	73
MSB002BR	36
MSB002CR	74
MSB 1C	54
MSB004BR	40
MSB004CR	57
MSB003BR	-
MSB003CR	69
MSB 39B	60
MSB 63B	31
SSM029B	53
Average	56
Median	57

Table 4. Specific Capacity and Efficiencies Calculated for RWM019.

Well ID	Test	Q (gpm)	Q/s GPM/ft	Well Efficiency (%)
RWM019	Step-Drawdown Test	49.4	2.81	87.5
		64.0	2.75	84.4
		79.4	2.62	81.3
RWM019	Long Term Test	79.1	2.27 ^a	70.0

^aAt end of 21-day pumping test.

Table 5. Well Loss Parameters Calculated for RWM019.

Well ID	Test	B (ft/ft ³ /min)	C (min ² /ft ⁵)	P
RWM019	Step-Drawdown Test	2.317	0.0501	2

Table 6 Aquifer Response to Step-Drawdown Test at RWM019.

Well Name	Distance from RWM019 (ft)	Maximum Drawdown During Step Test ¹ (ft)
RWM019	0	30.35
MSB 14A	263	2.52
MSB 14B	266	1.63
MSB002BR	323	1.32
MSB002CR	333	1.60
MSB 1C	338	1.96
MSB004BR	593	0.68
MSB004CR	600	0.68
MSB003CR	668	0.45
MSB003BR	674	0.00
MSB 39B	888	0.35
MSB 63B	1027	0.23
SSM029B	1930	0.00

¹At 79 gpm

Table 7. Maximum Drawdown as a Function of Days Since Start of Pumping for RWM019 Constant Rate Aquifer Test

Well ID	Maximum Drawdown after 5 Days Pumping (ft)	Maximum Drawdown after 13 Days Pumping (ft)	Maximum Drawdown after 19 Days Pumping (ft)	Distance from RWM019 (ft)
RWM019 ^a	- ^c	31.4	34.9	0
MSB14A	4.5	4.9	4.9	263
MSB14B	3.7	4.0	4.1	266
MSB002BR	2.3	2.6	2.6	323
MSB002CR	3.6	4.1	4.1	333
MSB001C	4.0	4.5	4.5	338
MSB004BR	1.5	1.8	1.8	593
MSB004CR	2.1	2.3	2.3	600
MSB003CR	2.0	2.3	2.3	668
MSB003BR	1.5	2.0	2.0	674
MSB39B	1.4	1.7	1.7	888
MSB63B	0.8	1.1	1.1	1027
SSM29B	0.5	0.7	0.7	1930

^aAverage flow 79.2 gpm

^bTurbulence in the well due to pumping made it difficult to obtain accurate water level readings.

Table 8 Flow Data from Recovery Well Network During Constant Rate Aquifer Test (as determined from ACP round sheets).

Well ID	Average Flow (gpm)	Median Flow (gpm)	Standard Deviation (gpm)
RWM 1	9	9	0.6
RWM 2	29	29	0.0
RWM 3	57	57	0.5
RWM 4	47	47	0.3
RWM 5	48	48	0.4
RWM 6	20	20	0.5
RWM 7	29	29	0.5
RWM 8	0	0	0.0
RWM 9	0	0	0.0
RWM 10	44	44	0.4
RWM018	0	0	0.0
RWM019	79	79	0.3

Table 9 RWM 1 Shutdown History.

Well ID	Date/Time	Elapsed ¹ Time (min)	Status	Flow (gpm)
RWM 1	8/26/2020 10:00	20220	Off	0
	8/26/2020 15:00	20520	On	9
RWM 1	8/29/2020 1:00	24000	Off	0
	8/31/2020 7:45	27285	On	10
RWM 1	9/1/2020 10:30	28890	Off	0
	9/1/2020 13:30	29070	On	10

¹Elapsed time since start of RWM019 pumping test (8/12/2020 09:00)

Table 10: Relative Well Dimensions Used in AQTESOLV Analysis of RWM019 Pumping Test Data.

	Distance from RWM019 (ft)	Depth Below GCCZ (ft)	Screen Length ¹ (ft)	Well Casing Radius ¹ (ft)	Effective Radius (ft)
RWM019	0	3.80	50.00	0.25	0.50
MSB 14A	263	36.49	20.00	0.17	0.33
MSB 14B	266	7.19	5.00	0.17	0.33
MSB002BR	323	43.31	10.00	0.08	0.17
MSB002CR	333	13.49	10.00	0.08	0.17
MSB 1C	338	35.09	4.70	0.17	0.33
MSB004BR	593	42.70	10.00	0.08	0.17
MSB004CR	600	13.07	10.00	0.08	0.17
MSB003BR	674	41.88	10.00	0.08	0.17
MSB003CR	668	13.79	10.00	0.08	0.17
MSB 39B	888	51.49	5.60	0.17	0.33
MSB 63B	1027	60.19	4.70	0.17	0.33
SSM029B	1930	36.24	10.00	0.08	0.17

¹As determined from BEIDMS well construction information.

Table 11 Hydraulic Properties of the Lost Lake Aquifer Based on Step-Drawdown Test at RWM019.

Well	Test Type	Transmissivity (ft ² /min)	Storativity	Leakage (r/B)	Aquifer Thickness (ft)	Hydraulic Conductivity (ft/day)
MSB14A	Step-Drawdown	1.1690	0.00020	0.1567	60.00	28.1
MSB14B	Step-Drawdown	1.8080	0.00044	0.0654	60.00	43.4
MSB1C	Step-Drawdown	0.9597	0.00062	0.0000	60.00	23.0
MSB002BR	Step-Drawdown	1.7250	0.00045	0.2347	60.00	41.4
MSB002CR	Step-Drawdown	2.4040	0.00013	0.0475	60.00	57.7
MSB003CR	Step-Drawdown	3.1690	0.00088	0.0000	60.00	76.1
MSB004BR	Step-Drawdown	2.0320	0.00061	0.3748	60.00	48.8
MSB004CR	Step-Drawdown	2.2440	0.00060	0.2453	60.00	53.9
MSB39B	Step-Drawdown	2.1730	0.00068	0.6749	65.00	48.1
MSB63B	Step-Drawdown	3.0140	0.00080	0.6707	65.00	66.8
Average		2.0698	0.0005	0.2470		48.7
Median		2.1025	0.0006	0.1957		48.5
Standard Deviation		0.7059	0.0002	0.2543		16.2

Table 12 Hydraulic Properties of the Lost Lake Aquifer Based on Constant Rate Pumping Test at RWM019.

Well	Test Type	Transmissivity (ft ² /min)	Storativity	Leakage (r/B)	Aquifer Thickness (ft)	Aquifer Hydraulic Conductivity (ft/day)	Aquitard Thickness (ft)	Aquitard Hydraulic Conductivity (ft/day)
MSB14A	Constant Rate	1.3540	0.0002	0.0195	60	32.5	4	4.3E-05
MSB14B	Constant Rate	1.2100	0.0011	0.0549	60	29.0	4	3.0E-04
MSB001C	Constant Rate	1.0930	0.0006	0.0575	60	26.2	4	1.8E-04
MSB002BR	Constant Rate	2.3940	0.0004	0.0287	60	57.5	4	1.1E-04
MSB002CR	Constant Rate	1.3650	0.0005	0.0352	60	32.8	4	8.8E-05
MSB003BR	Constant Rate	0.5498	0.0059	0.7169	60	13.2	4	3.6E-03
MSB003CR	Constant Rate	1.3400	0.0016	0.1747	60	32.2	4	5.3E-04
MSB004BR	Constant Rate	2.5770	0.0007	0.0686	60	61.8	4	2.0E-04
MSB004CR	Constant Rate	1.7480	0.0008	0.0948	60	42.0	4	2.5E-04
MSB39B	Constant Rate	2.0770	0.0012	0.1087	65	46.0	4	1.8E-04
MSB63B	Constant Rate	3.2980	0.0014	0.1346	65	73.1	4	3.3E-04
SSM29B	Constant Rate	1.3390	0.0027	0.7570	60	32.1	4	1.2E-03
Average		1.6954	0.0014	0.1876		39.9		8.0E-05
Median		1.3595	0.0010	0.0817		32.6		2.2E-04
Standard Deviation		0.7611	0.0016	0.2607		17.0		1.0E-03

Table 13. Average Hydraulic Properties of the Lost Lake Aquifer Near RWMO19

	Transmissivity (ft ² /min)	Hydraulic Conductivity (ft/day)	Storativity	r/B	Green Clay Hydraulic Conductivity (ft/day)
Average	1.8656	43.9	0.0010	0.2146	1.7E-03
Median	1.7780	42.7	0.0007	0.1018	3.1E-04
Standard Deviation	0.7439	16.8	0.0012	0.2534	2.4E-03

Distribution:

branden.kramer@srs.gov

joao.cardoso-neto@srs.gov

john02.bradley@srs.gov

larry.mullikin@srs.gov

j.ross@srs.gov

thelesia.oliver@srs.gov

dennis.jackson@sml.doe.gov

brady.lee@sml.doe.gov

Records Administration (EDWS)